RESULTS & DISSCUSION

CHAPTER III

Results and Discussion

Corrosion inhibition of C-steel in acid chloride solution by some indole derivatives

It is generally accepted that organic compounds inhibit corrosion by adsorbing at the metal / solution interface. However, the modes of adsorption are dependent on: a) chemical structure of the molecule, b) chemical composition of the solution, c) nature of the metal surface, and d) electrochemical potential at the interface, one or a combination of more of the three principal types of adsorption: π bond, electrostatic and / or chemisorption [160]. In addition, it is believed that the formation of a solid organic molecule complex with the metal atom has received considerable attention [161].

When designing inhibitors, all of the theories are in common agreement that adsorption phenomena involves either: 1) proton acceptor (cathodic site absorbers), materials in this group accept the hydrogen ions or proton and migrate to the cathode. 2) electron acceptor (anodic site absorbers) inhibitor functions due to their ability to accept electrons. 3) adsorb at anodic and cathodic sites .It has been generally accepted that group contributions vary considerably from molecule to molecule. Utilization of these concepts permits the systematic construction of increasing the efficiency of organic molecule.

Indole derivatives were selected for corrosion inhibition of C-steel of petroleum pipes in acid chloride solutions. The effect of the concentration of inhibitors was studied by weight-loss measurements and polarization technique at temperature of 30°C.The correlation between inhibitor structure and molecular charge in a given position depends heavily upon

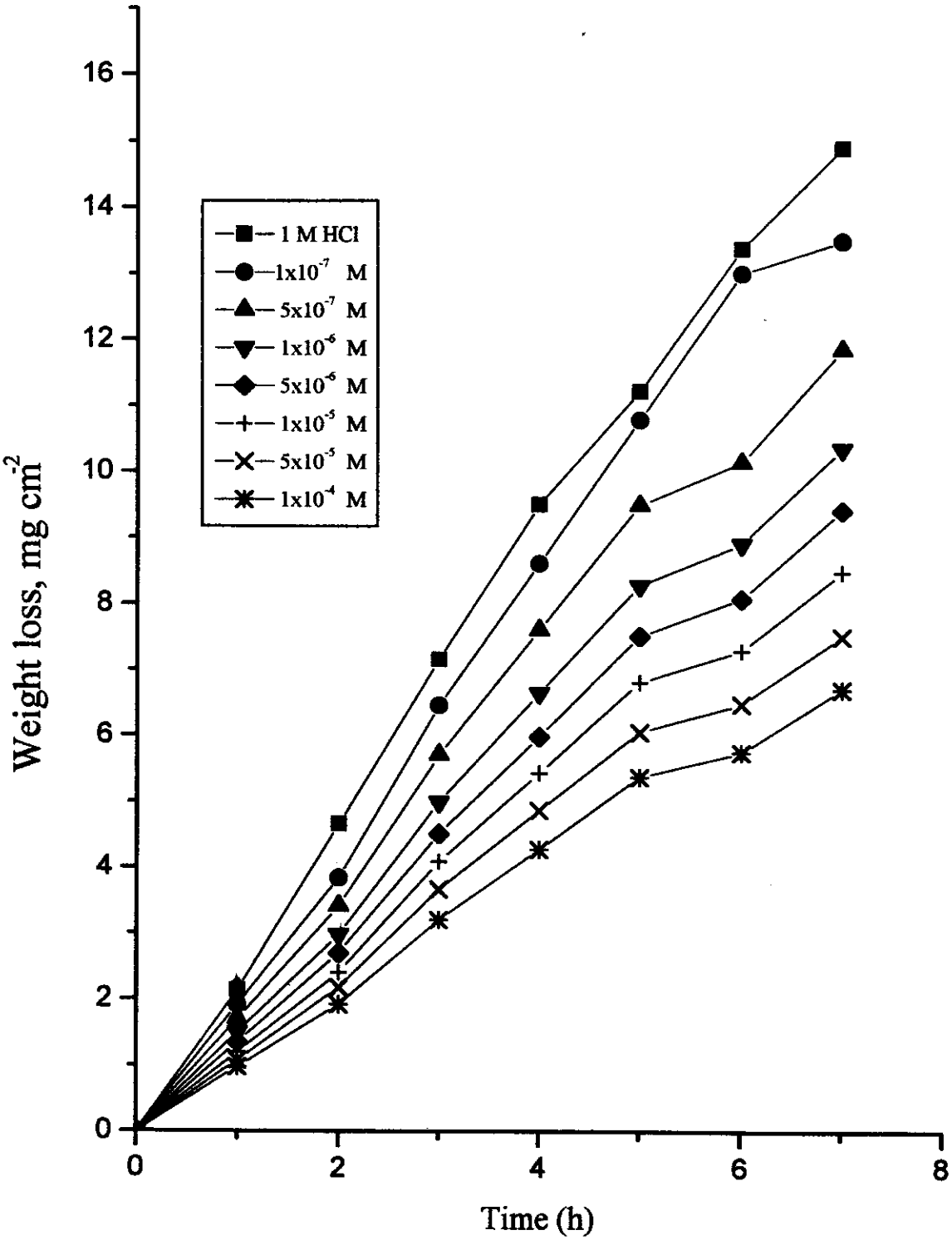

Fig. (3.1): Weight loss-time curves for C-steel dissolution in 1 M HCl in The absence and presence of different concentrations of inhibitor (I)

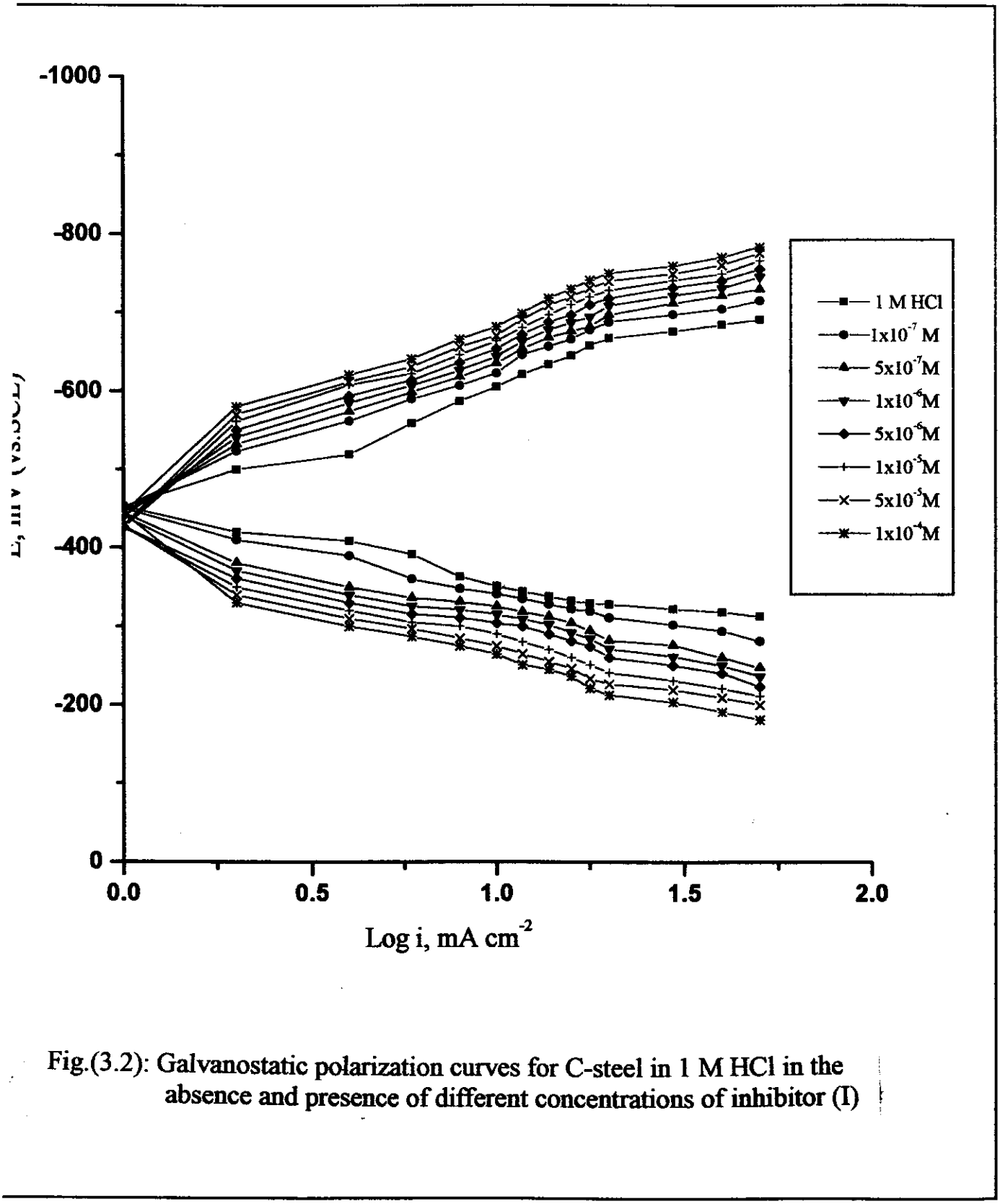

Fig.(3.2): Galvanostatic polarization curves for C-steel in 1 M HCl in the absence and presence of different concentrations of inhibitor (I)

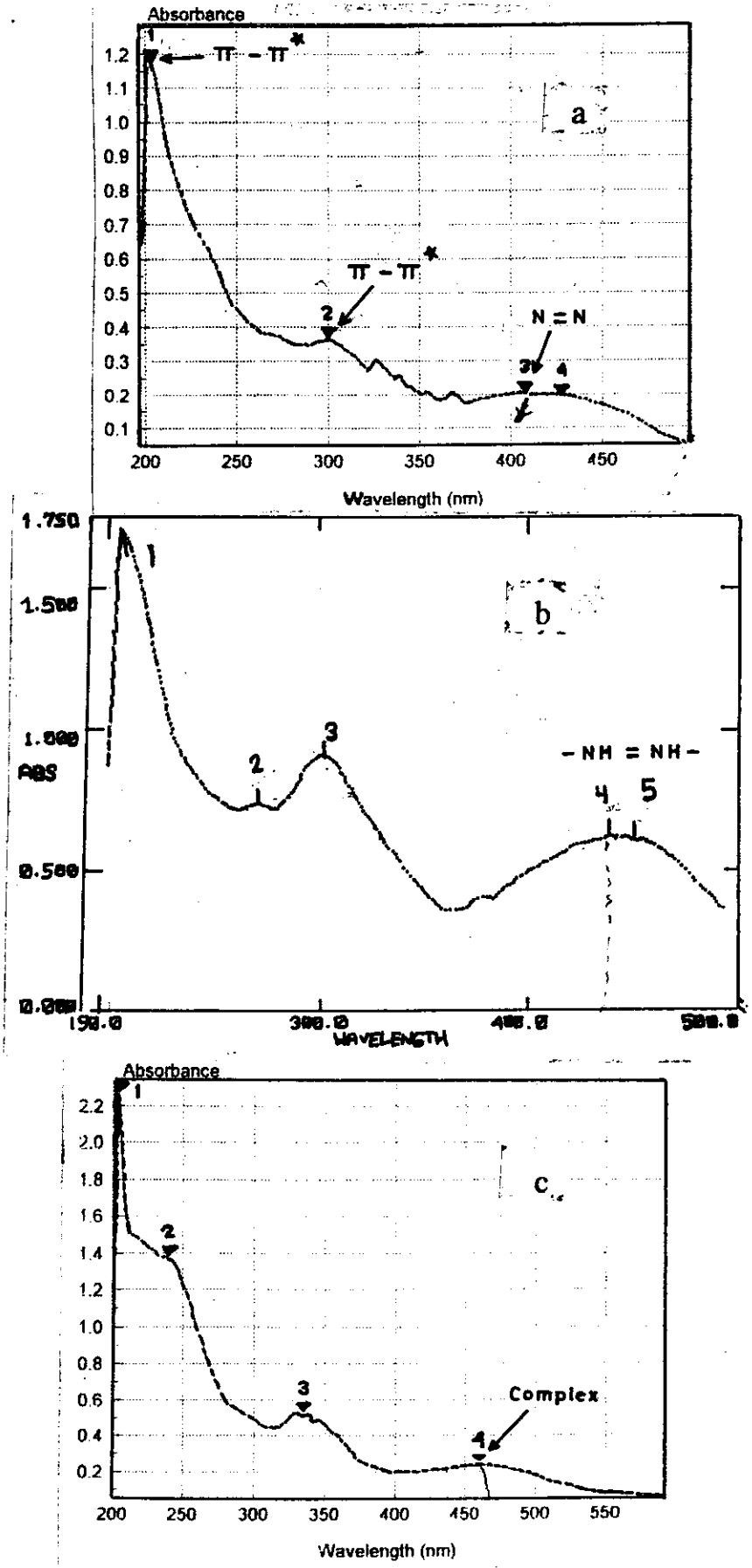

Fig. (3.3): Absorbance- wave length curves for 4-phenylazo-2-(indol-2-yl) phenol in absence (a) and presence (b) of 1M HCl and (c) 1 M HCl + Fe^{2+}

It can be considered as the Volmer reaction [164].

$$[\,Fe\,H^{+}\,]_{ads.} + e = [\,FeH\,]_{ads.} \qquad (3.2)$$

Followed by the Heyrovsky reaction.

$$e + Fe_{M} + [H_3O]^{+} + H_{ads.} = Fe_{M} + H_2O + H_2 \qquad (3.3)$$

The rate of these reactions will be governed by the availability of electrons at the cathodic site. The azo group of the inhibitor molecule is reduced by the discharged hydrogen and causes change in the solution colour from yellow to faint yellow or colorless. The reduced species can inhibit also the corrosion process.

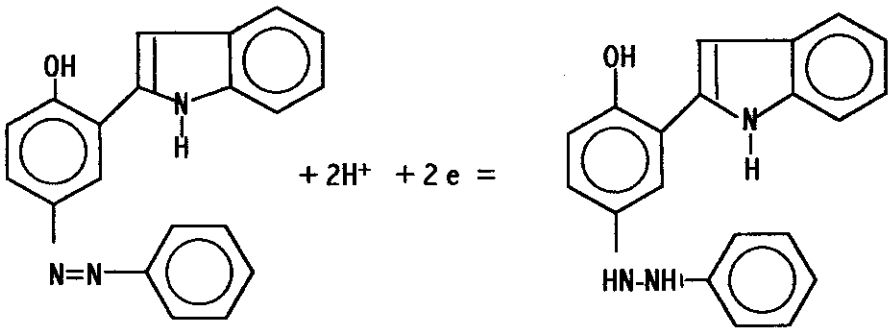

Reduced form

The study of electronic spectra can be helpful in predicting the nature of the inhibitor after its reduction [165]. The inhibitor used in this work is 4-phenylazo-2- (indol-2 -yl) phenol. Its electronic spectrum, (Fig3.3) shows a relatively intense broad band with a maximum at 408 nm, which is characteristic of the azobenzene group. Two other $\pi \longrightarrow \pi^{*}$electronic transitions appear around 203 and 300 nm, respectively.

The spectrum of the inhibitor after reduction is very much similar to that before reduction except for the significant decrease of the intensity of the longest wavelength band. This result is an evidence that the azo group, -N = N-, has been reduced to hydrazine, -NH - NH-, without bond breaking. Also this can be confirmed by the increase in the wavelengths by reduction (λ = 439 nm) and by complexation(λ=460 nm) this is due to the reduction of the ionization energies. Phenylhydrazine long wavelength transition

(λ=250 nm) does not appear in the spectrum of the inhibitor after reduction. The spectrum of the inhibitor after reduction is an evidence that, bond breaking does not take place on reduction.

The protective efficiency and the degree of surface coverage of the inhibitor would increase by increasing the inhibitor concentration. The effect of substituted groups, e.g., $-CH_3$, $-OCH_3$, $-NO_2$, and also its position (ortho-, meta-, para-), will be discussed later in details.

ii) Effect of substituted group:

As shown previously that the inhibition process depends essentially on the electron density at the active centers of the inhibitor molecule. The subsequent step is to follow the effect of substituted group whether increases or decreases the inhibition efficiency through its effect on the active centers, i.e., electron donating or withdrawing groups, e.g., alkyl, alkoxyl and nitro. The three substituted groups studied are, methyl, methoxy and nitro which located in para , meta and ortho position of phenyl ring with respect to the phenylazo molecule derivatives . The inhibition effect of such derivatives was compared with that of the parent compound (I) using weight-loss and galvanostatic polarization measurements. The result of corrosion potential $E_{corr.}$[166], surface coverage calculated using equation (3.4) and (3.5) for each technique ,θ and θ_i and anodic and cathodic Tafel slope,[β_a &β_c]are listed in Tables (3.1 – 3.10) .

From weight-loss measurements.

$$\theta = (1 - \frac{\Delta w_{inh.}}{\Delta w_{free}}) \qquad (3.4)$$

and from polarization measurements :

$$\theta_i = (1 - \frac{i_{inh.}}{i_{free.}}) \qquad (3.5)$$

The percentage inhibition is calculated from surface coverage, thus:

$I\% = \theta \times 100$ or (3.6)

$= \theta_i \times 100$ (3.7)

Weight-loss of C-steel in mg cm^{-2} of the surface area was determined in an open system at various time intervals in absence and presence of indole derivatives. The obtained weight-loss time curves are represented in Figs. (3.4 - 3.12). The inhibition efficiency of corrosion was found to be dependent on the inhibitor concentration, nature of substituents and their positions in indole derivatives. Data of Table (3.11) show that, the order of increasing inhibition efficiency of C-steel in 1M HCl by the different substituted groups as obtained from galvanostatic technique follows:

Unsubstituted $< -NO_2 < -CH_3 < -OCH_3$

The variation of surface coverage as determined from weight-loss measurments, θ , with the logarithm of the inhibitor concentration are represented in Figs.(3.13 - 3.22), (and of S- shape obeying the Frumkin adsorption isotherm [30] and is in good agreement with the Frumkin equation (1.2)). As shown from these figures, one can conclude that the degree of surface coverage increases as the concentration of the inhibitor increases and hence, the inhibition efficiency increases.

Anodic and cathodic polarization were carried out galvanostatically in unstirred 1 M HCl in presence and absence of various concentrations of the inhibitors at 30 °C. At all current densities, during polarization, the overpotentials were slightly shifted with time and then attained steady values. These steady overpotential values were used for the construction of anodic and cathodic Tafel plot. The results are represented in Figs. (3.23 - 3.31). These results indicate that, the presence of indole derivatives in solution inhibits both the hydrogen evolution and the anodic desolution processes .The indole derivatives induce a decrease in $I_{corr.}$ values. This

indicates that these compounds act as inhibitors. The results of Tables (3.1—3.10) indicate that the inhibition efficiency in general depends on the inhibitor concentration, nature of substituent and its position in the indole derivatives. The results also show that the slopes of the anodic and the cathodic Tafel lines (β_a, β_c) were slightly changed on increasing the concentration of the tested compounds. This indicates that there is no change of the mechanism of inhibition in presence and absence of inhibitors. The indole derivatives are mixed – type inhibitors, but the cathode is more polarized than the anode when an external current was applied. The higher values of Tafel slopes can be attributed to surface kinetic process rather the diffusion-controlled process.[167].

On the light of the previous discussion, the nature of substituted group, whether electron donating or withdrawing, reflects its effect on the inhibition efficiency .One can say that the methyl and methoxy groups increase the electron density on the active centers, consequently, the inhibition efficiency increases. It follows that the methoxy group is more efficient than the methyl one. From structural organic point of view, both methyl and methoxy groups have + R effect but the inductive effect is + I and –I, respectively. Although the methyl group has +R, but its effect is very little as a result of hyperconjugation, thus:

In the case of methoxy group, the effect of +R is large and also the inductive effect, -I, thus:

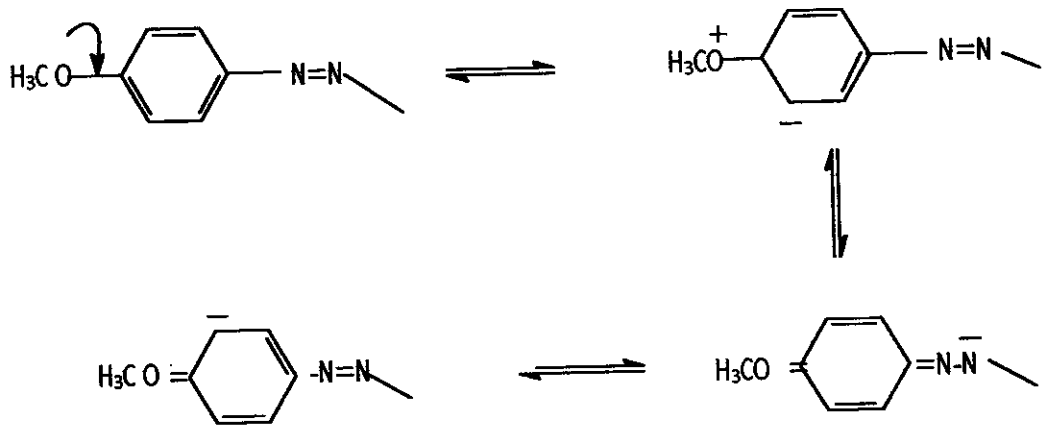

Also methoxy group may add an additional active center and this increases the inhibition efficiency in case of methoxy group than in case of methyl group.

On the other hand, the low efficiency of nitro derivatives than methyl and methoxy derivatives may be due to:

i) Its highest electrophilic character ii) its easily reduction in acid medium and iii) the evolved heat of hydrogenation may aids the desorption of the molecules.

In addition inhibitor (I) is the least efficient inhibitor, this is due to the absence of any substituent groups.

A skeletal representation of the proposed mode of adsorption of the studied compounds is shown in Fig. (3.32) and clearly indicates the active adsorption centers.

In a similar manner to Hammett equation, one can correlate the corrosion current ($I_{corr.}$) with the substituent Hammett constants (σ) of the substituted group, c.f. Table (3.12). Such plots are shown in Fig. (3.33)

Table (3.12). -

Substituent	Substituent constants ,σ	
	para - position	meta- position
Methyl	- 0.17	- 0.07
Methoxy	- 0.27	+ 0.12
Nitro	+ 0.78	+ 0.71

As obvious from Fig. (3.33), the variation is linear and obeys the following equation:

$$I_{corr.} = \rho\sigma \qquad (3.8)$$

where ρ is the proportionality constant, which depends on the nature of both the metal under investigation and the electrolyte solution. It is a measure of the sensitivity of a given series of inhibitor compounds to impart inhibition action. Also, it is clear that the slopes of straight line for (ortho & para) substituted groups are nearly identical.

One further point remains which is the colour of studied solutions of different derivative changes to coluorless for low inhibitor concentrations. This is due to its reduction. The presence of inhibitor molecule in both forms of non- and reduced form acts as an inhibitor for acid chloride corrosion of C-steel.

iii) Effect of substituent position:

As obvious from the previous discussions that corrosion inhibition of C-steel in acid chloride solution was found to depend on the type of substituted group as well as its position with respect the functional azo group. This part deals with the effect of substituent position, para-, mata-, or ortho- for each substituted group.

The data of weight loss, corrosion current, $I_{corr.}$, and surface coverage θ and θ_i ,calculated from weight loss and polarization

measurements for different substituent positions shows that the inhibition efficiency follows the following order : para-< meta- < ortho-

In view of the above results deduced by galvanostatic polarization and weight-loss, the o-substituted derivatives for all investigated substituted groups, CH_3-, OCH_3- or NO_2- occupies a distinct position for inhibition efficiency. From the structural organic point of view, the location of substituent group in the ortho – position has both inductive and resonance effects which may operate together strongly and there is no effect of steric hinderance, because the large distance between centers of adsorption and the substituent group. When the substituent is in the meta-position, the inductive effect affect only, due to the alternating system of atom in the conjugate system, resonance effect become less or nearly disappears. In case in which the substituent group is located in the para-position, the inductive effect is relatively small owing to the presence of four carbons distant.

Generally, one can conclude that the inhibition efficiency of indole derivatives depends on substituent group type and its position with respect to azo group, and also on the inhibitor concentration. The order of increasing efficiency for different substituent groups follows: unsubstituted ($\sigma = 0.0$) < -NO_2, ($\sigma = 0.78$) < –CH_3 ($\sigma = -0.17$)< –OCH_3 ($\sigma = -0.27$) and for group position para-< meta- < ortho-

(iv) Effect of temperature:

In this part the effect of temperature on both corrosion and corrosion inhibition of C-steel was studied. The behaviour in 1 M HCl solutions at different temperature range of 30 – 55°C was investigated by weight- loss measurement for a constant time period of 7 hours. Arrhenius plot of logarithm of corrosion rate, log K, with reciprocal of

absolute temperature, 1/T, is shown graphically in Figs. (3.34 –3.43) for C-steel in the presence of $1x10^{-4}$, $1x10^{-5}$and $1x10^{-6}$ M and absence of inhibitors.

As obvious from these figures, the increase of temperature activates the corrosion reaction and consequently, the rate of corrosion increases. The variation of log K vs. 1/T is a linear one which obey 's the following equation:

$$\ln K = B - \frac{Ea}{RT} \qquad (3.9)$$

where B is a constant depends on the metal type and electrolyte. The activation energy, Ea, calculated from the slope, Ea /R, is equal to 21.1 KJ mol^{-1}.El-Morsi[167],found that the activation energy is 33.84 KJ mol^{-1}, for steel in 0.5 M HCl solution but Fouda [168],found it to be 63.56 KJ $mol^{-1}$for C-steel in 2M HCl solution, On the other hand, Mathur [169], found that the activation energy of iron in 0.6 M HCl is equal to 61.15 KJ $mol^{-1}$and in 0.4 M H_2SO_4 is equal to 64.1 KJ mol^{-1}. Generally, one can say that the nature and concentration of the electrolyte and the type of metal affect greatly the activation energy for the corrosion process.

Inspection of the data given in Table (3-16) shows that:

i) For one and the same group E_a decreases in the order ortho> meta >para .

ii) For the same substitution position E_a is increased in order,

free acid < I < II < III < IV

On the other hand, the effect of temperature on inhibition efficiency of the inhibitor II, III, IV at 10^{-4}- 10^{-6} M were investigated by weight- loss measurement at different temperature 30 – 55°C. As clear from Tables (3.13- 3.15) that inhibition efficiency depends on the

inhibitor concentration, position of the substituent and solution temperature. At temperatures studied, the inhibition efficiency increases with increasing the concentration at one hand and decreases with rise of temperature on the other hand. From the results of the effect of temperature, it was observed that the inhibition efficiency decreases with increasing temperature. This means that these compounds are adsorbed physically on carbon steel surface.

Table (3.16) includes the values of apparent activation energy, entropy and enthalpy of activation of corrosion of C-steel in 1M HCl in the absence and presence of inhibitors.

Enthalpy and entropy of activation ($\Delta H°$, $\Delta S°$) were calculated from transition state theory [170].

$$K = \frac{RT}{Nh} \exp^{(\Delta S°/R)} \exp^{(-\Delta H°/T)} \qquad (3.10)$$

Where h is Plank's constant, N is Avogadro's number, R is the universal gas constant, $\Delta H°$ is the enthalpy of activation and $\Delta S°$ is the entropy of activation .A plot of log K/T vs. 1/T (equation 3.10) also gave straight lines as shown in Figs. (3.44 – 3.47). The slopes of these lines equal $\Delta H°$ /2.303 R and the intercept equal log RT/ Nh + ($-\Delta S°$/2.303 R) from which the value of Δ? °and $\Delta S°$ were calculated (Table 3.17).$E°_a$ and $\Delta H°$ of the inhibition process of C-steel in 1 M HCl in the presence of inhibitors are nearly the same (or slightly higher) as those in free 1 M HCl solution, indicating that no energy barrier is attained [172]. These data reveal that the inhibition of the corrosion reactions is affected without changing the mechanism .The entropy of activation in the presence and absence of the inhibitor is large and negative. This implies that the activated complex in the rate-determing step represents

association rather than dissociation, , indicating that a decrease in disorder takes place in going from reactant to the activated complex.

The reaction temperature does not affect the order of inhibition efficiency of different additives as gathered from the increase in the activation energy. The order of increasing inhibition efficiency for the inhibitors used is: unsubstituted $< -NO_2 < -CH_3 < -OCH_3$ and for the substituted position: - para <–meta<–ortho.

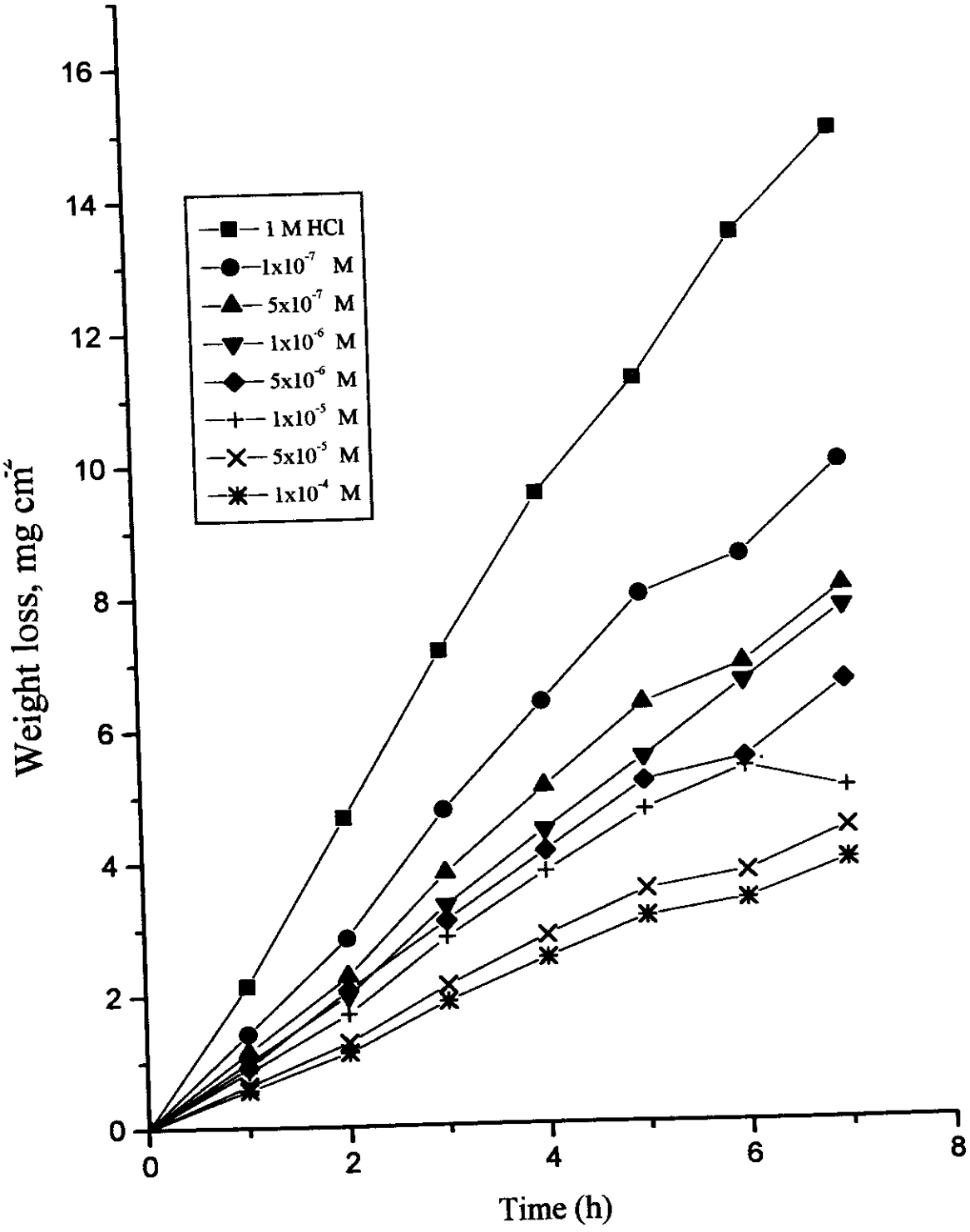

Fig. (3.4): Weight loss-time curves for C-steel dissolution in 1 M HCl in The absence and presence of different concentrations of inhibitor (II-a)

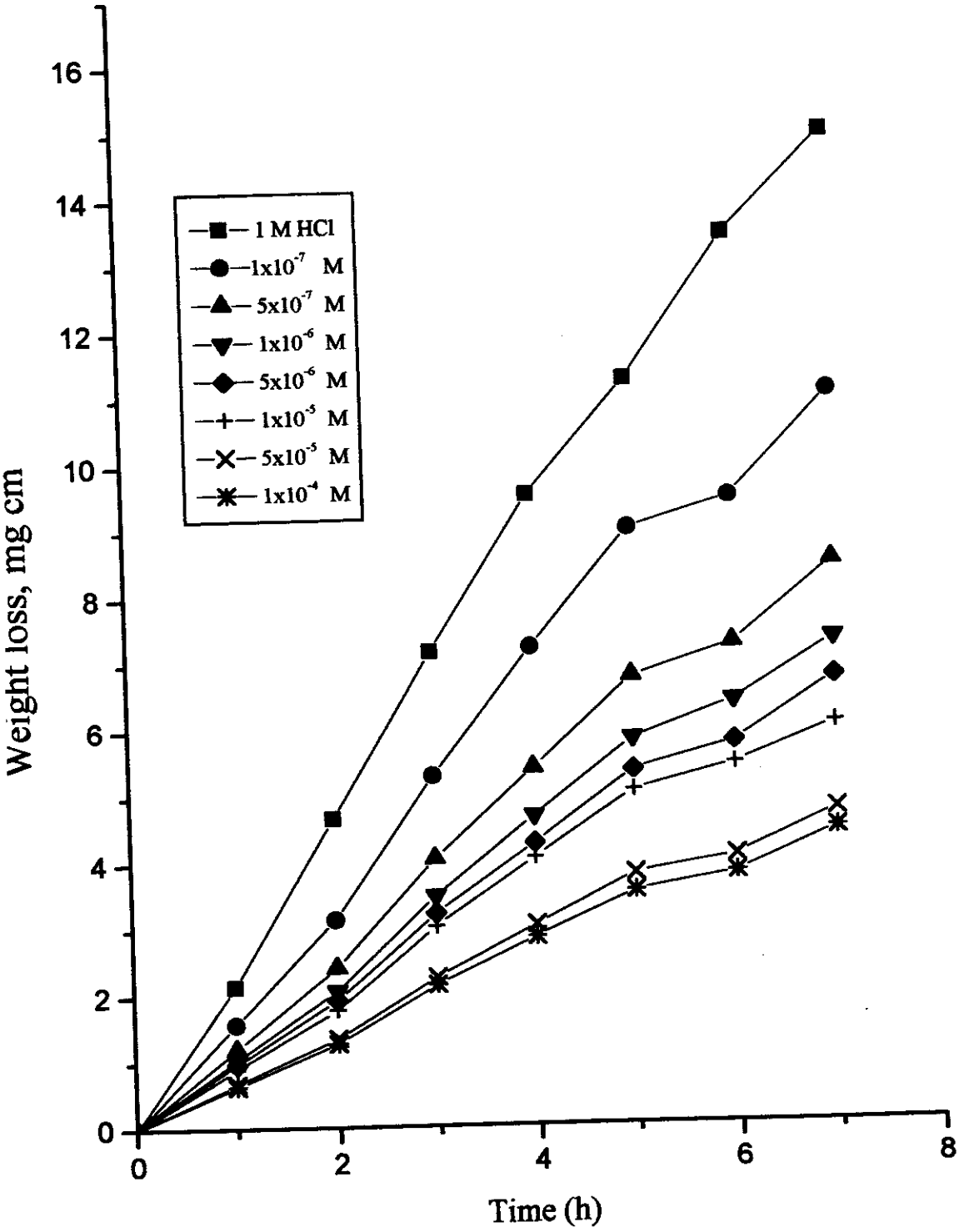

Fig. (3.5): Weight loss-time curves for C-steel dissolution in 1 M HCl in The absence and presence of different concentrations of inhibitor (II-b)

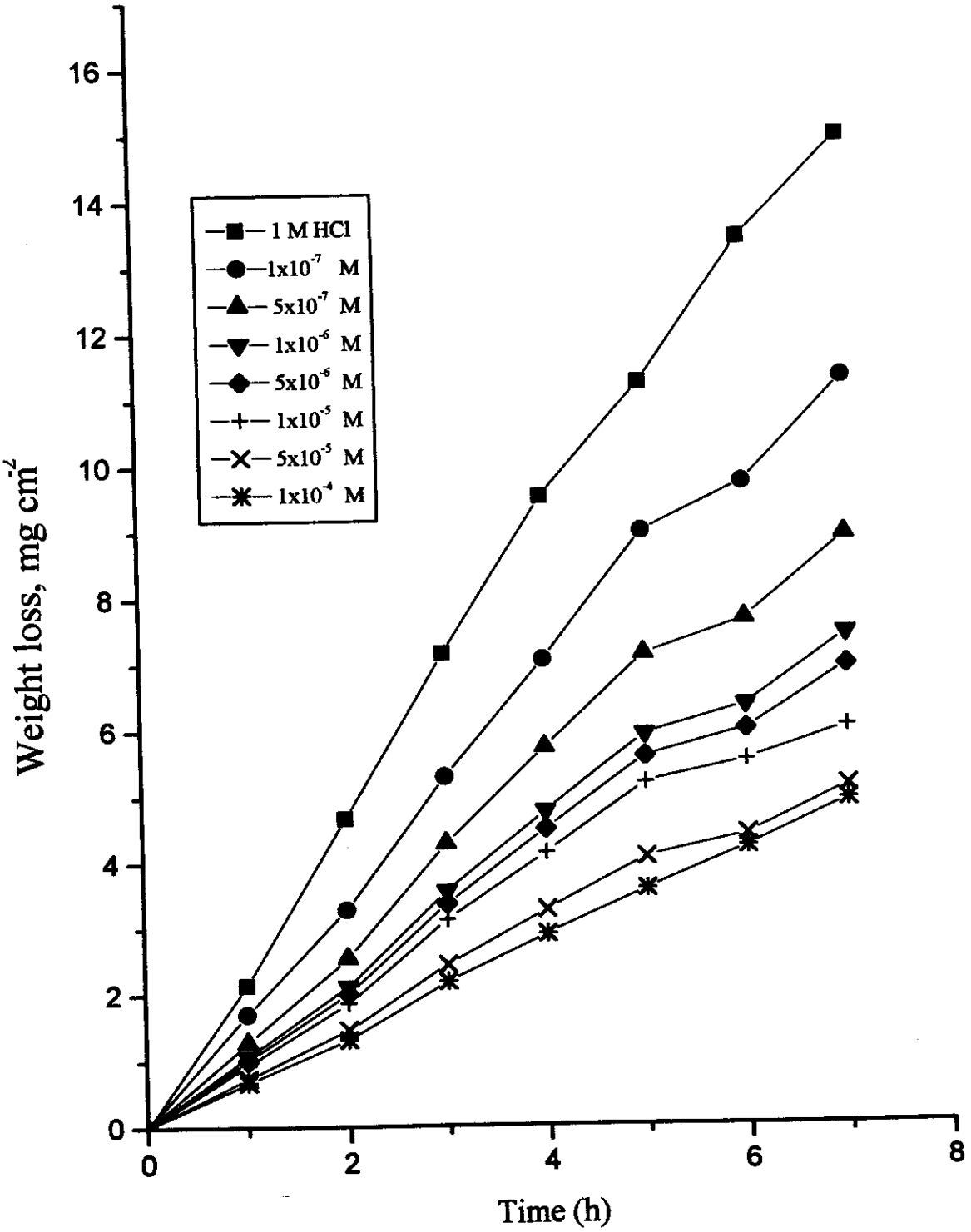

Fig. (3.6): Weight loss-time curves for C-steel dissolution in 1 M HCl in The absence and presence of different concentrations of inhibitor (II-c)

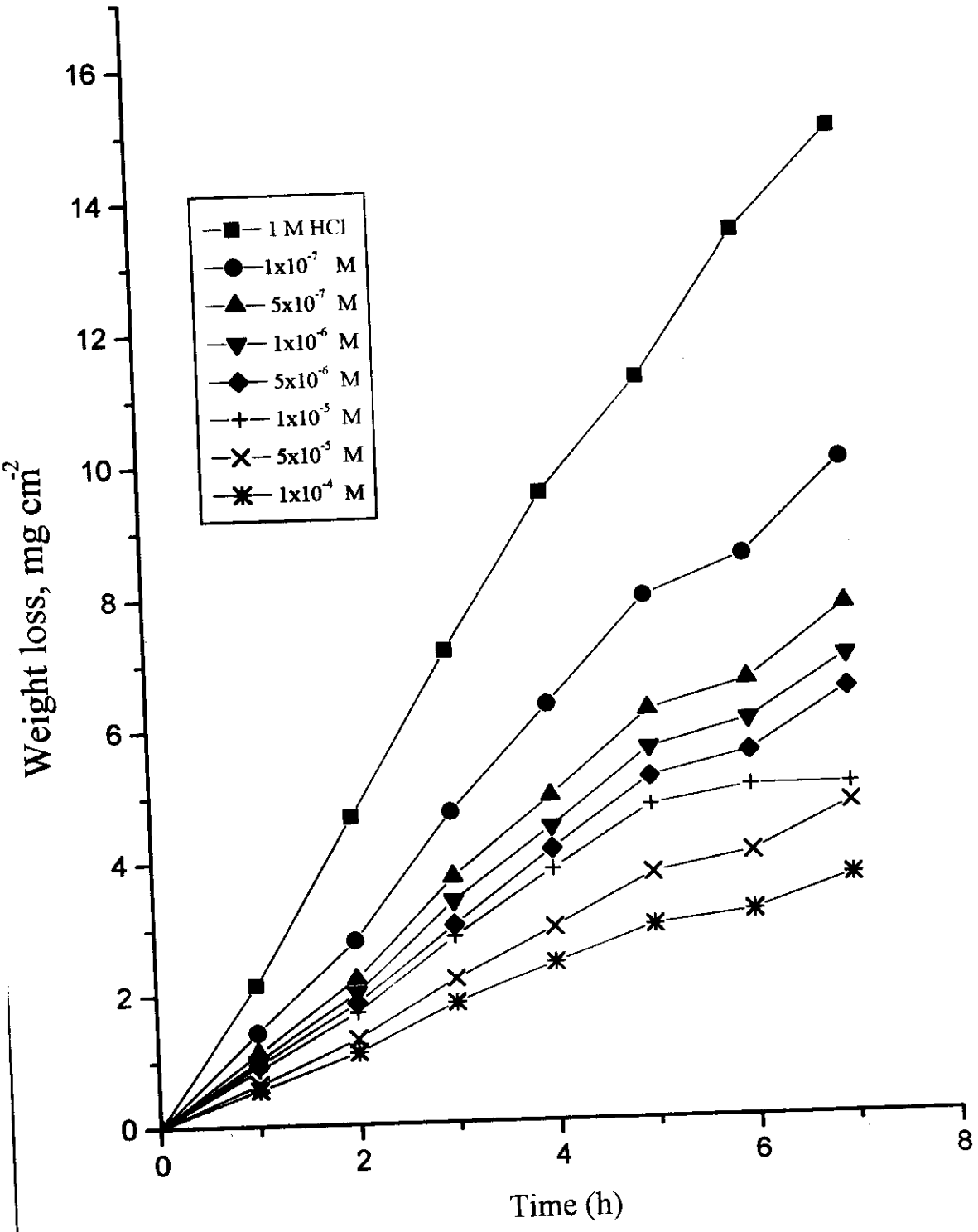

Fig. (3.7): Weight loss-time curves for C-steel dissolution in 1 M HCl in The absence and presence of different concentrations of inhibitor (III-a)

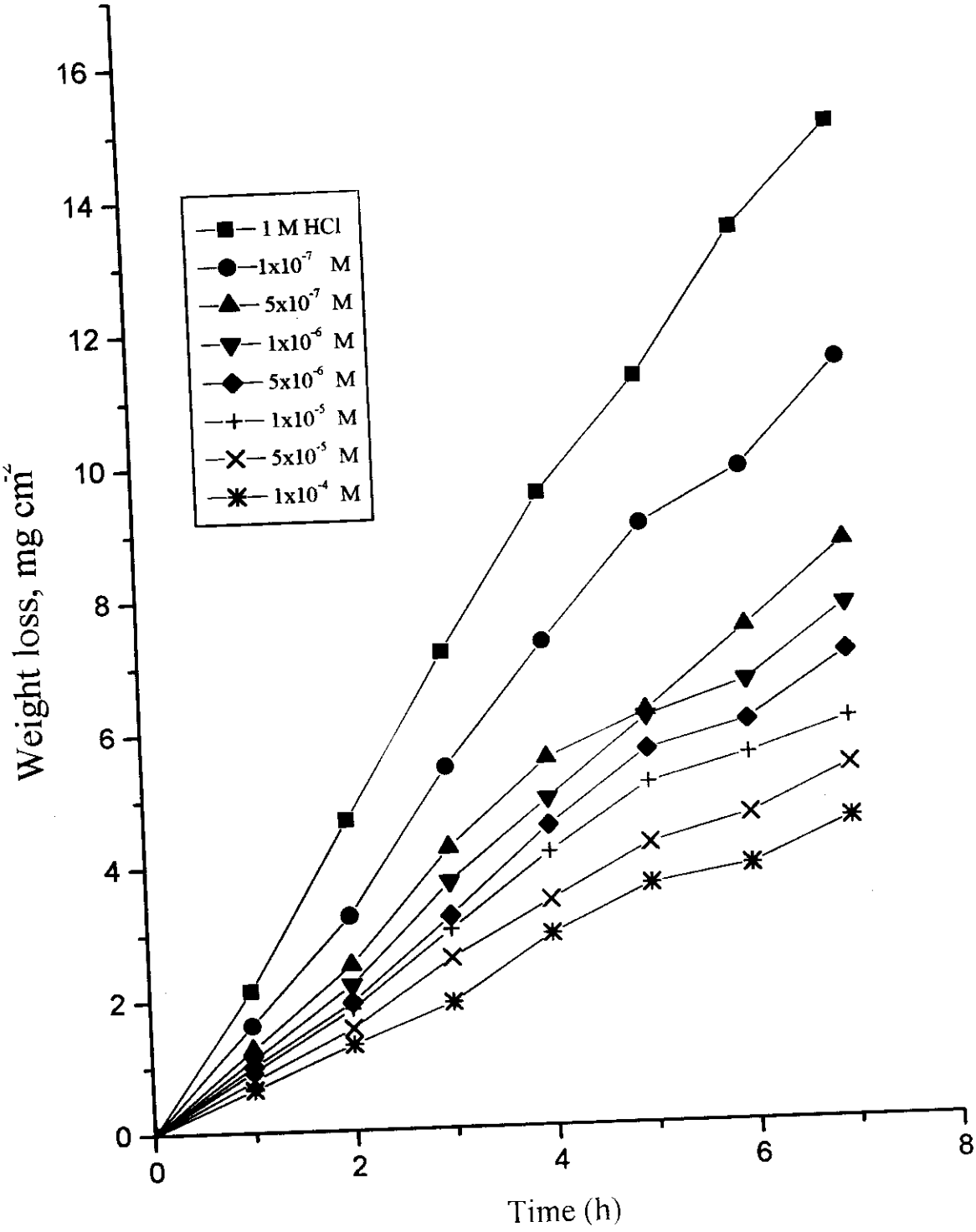

Fig. (3.8): Weight loss-time curves for C-steel dissolution in 1 M HCl in The absence and presence of different concentrations of inhibitor (III-b)

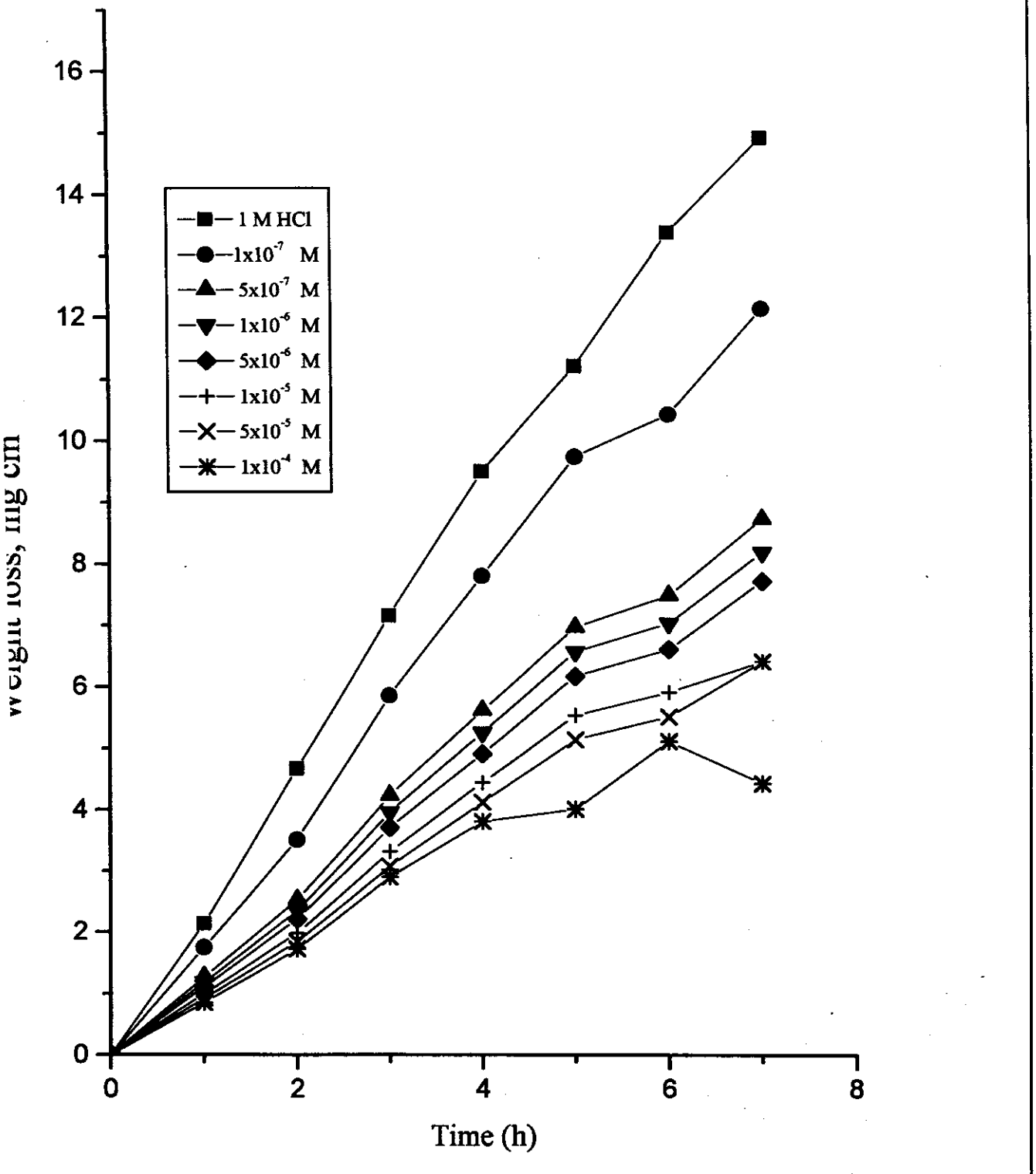

Fig. (3.9): Weight loss-time curves for C-steel dissolution in 1 M HCl in The absence and presence of different concentrations of inhibitor (III-c)

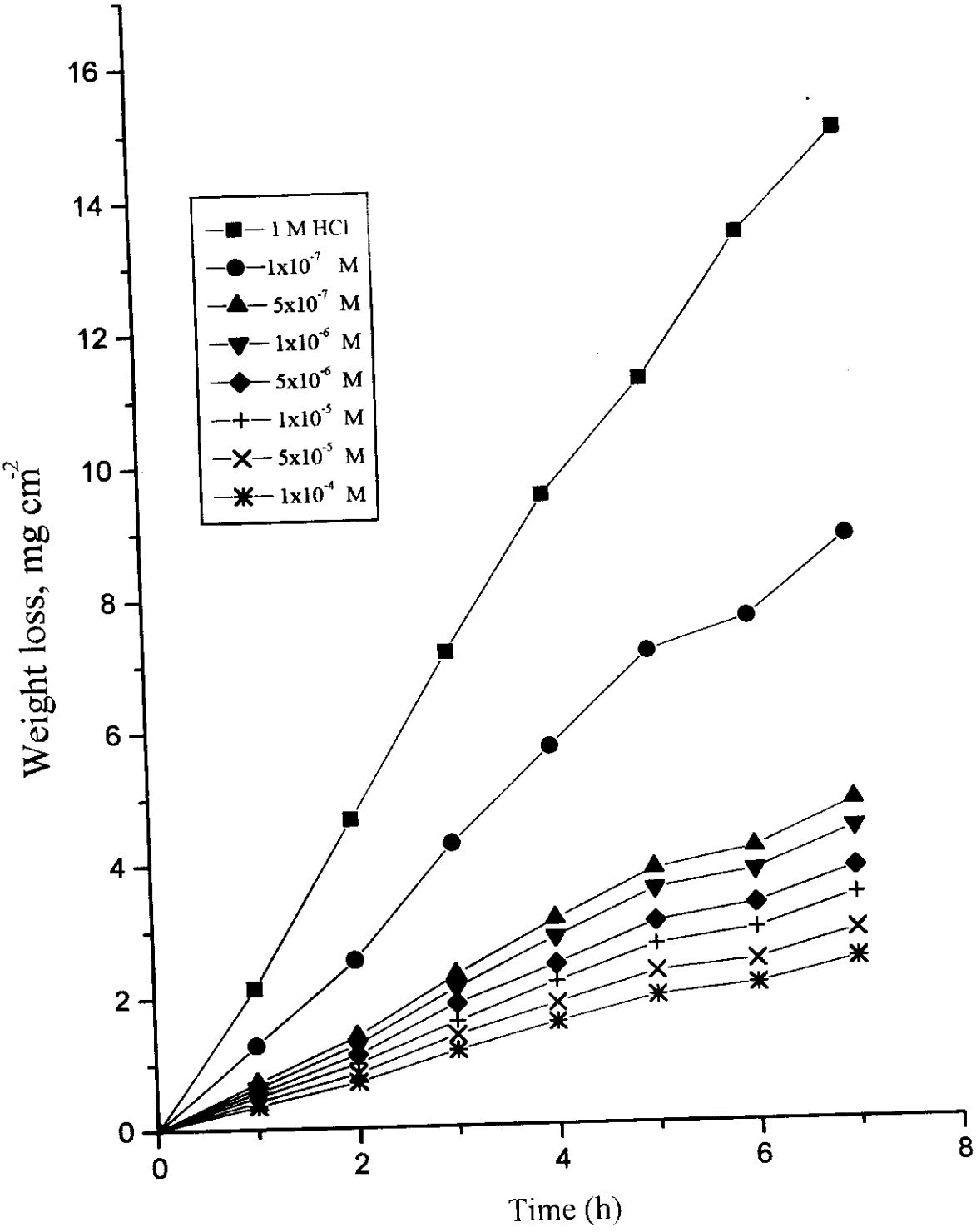

Fig. (3.10): Weight loss-time curves for C-steel dissolution in 1 M HCl in The absence and presence of different concentrations of inhibitor (IV-a)

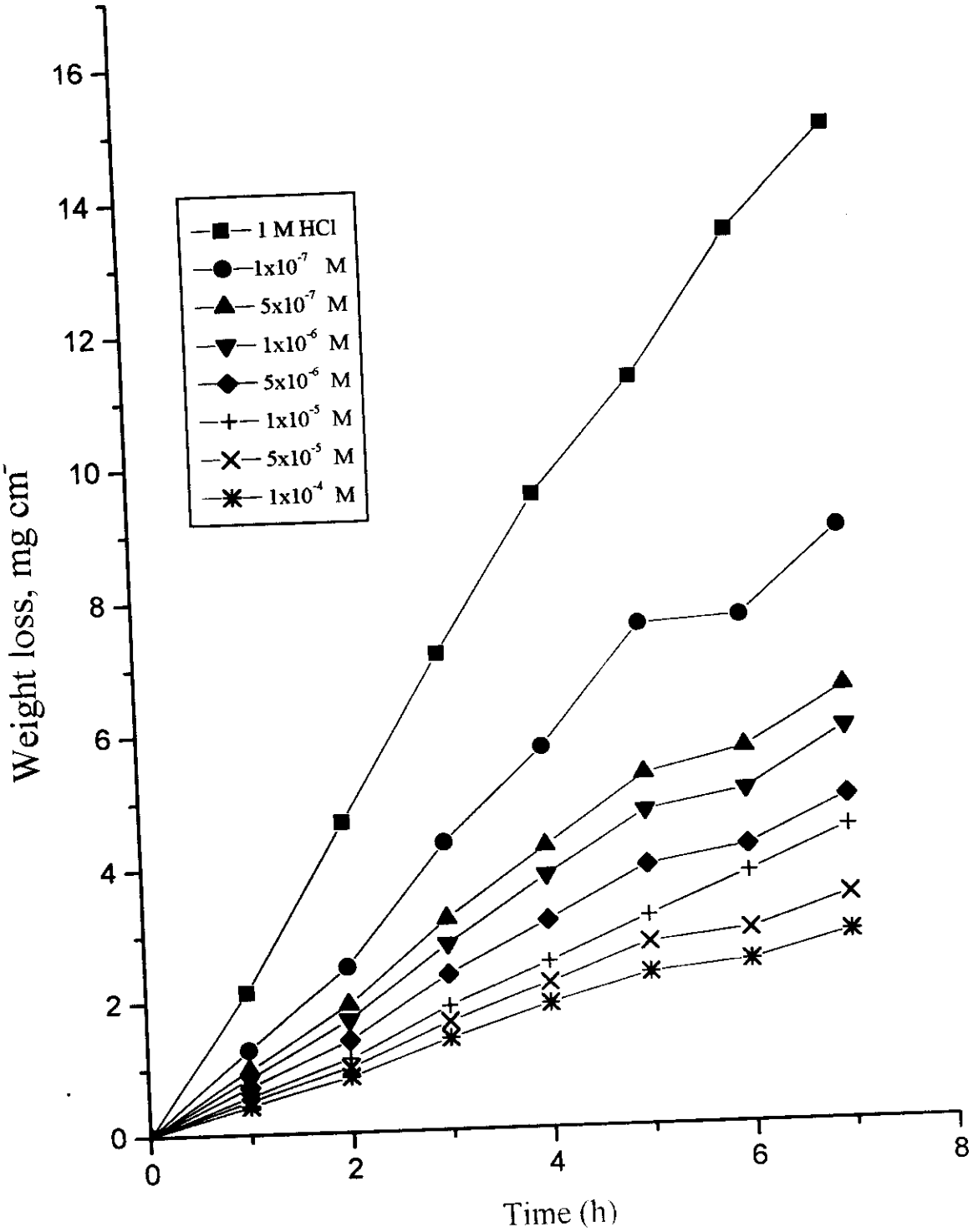

Fig. (3.11): Weight loss-time curves for C-steel dissolution in 1 M HCl in The absence and presence of different concentrations of inhibitor (IV-b)

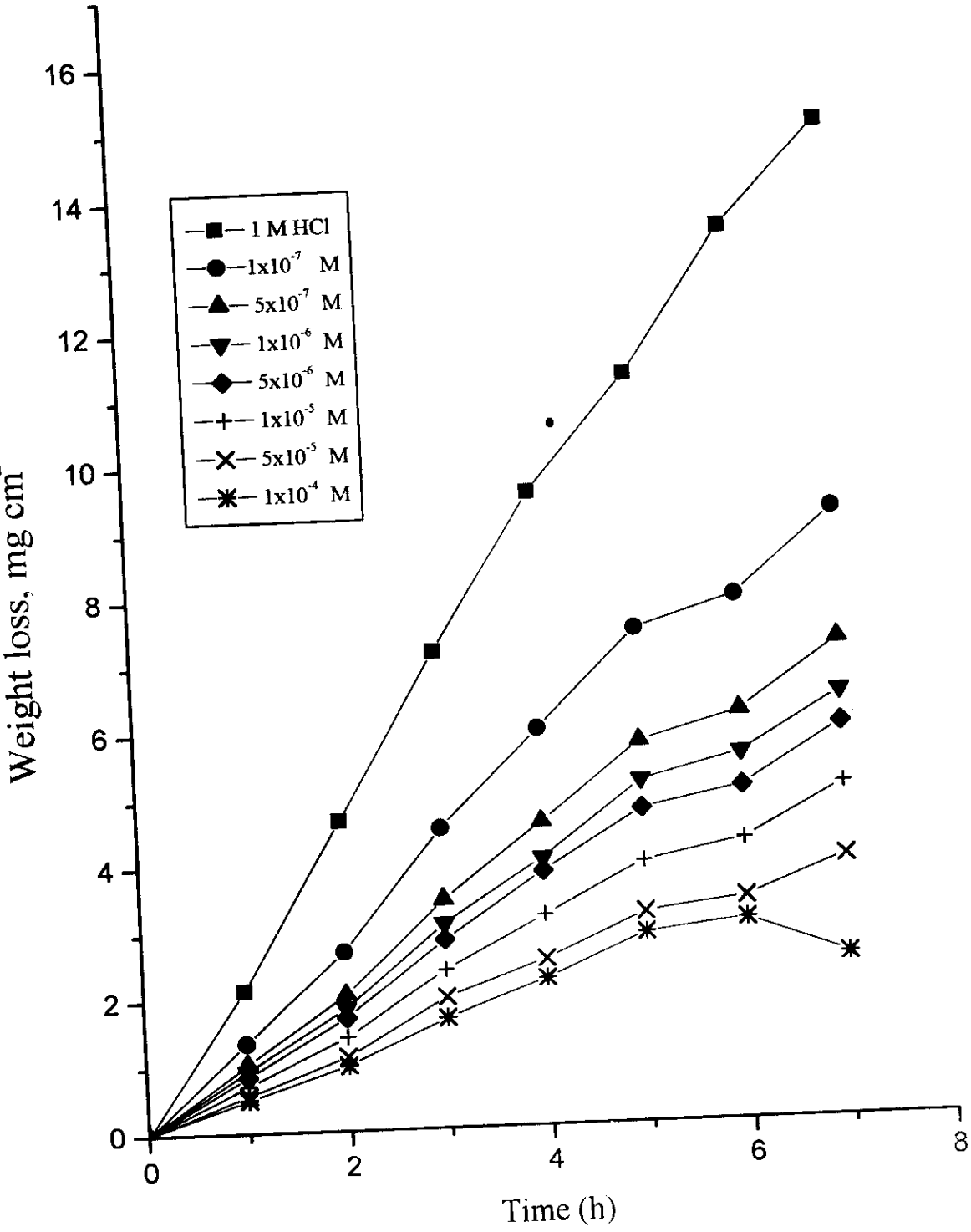

Fig.(3.12):Weight loss-time curves for C-steel dissolution in1M HCl in The absence and presence of different concentrations of inhibitor (IV-c)

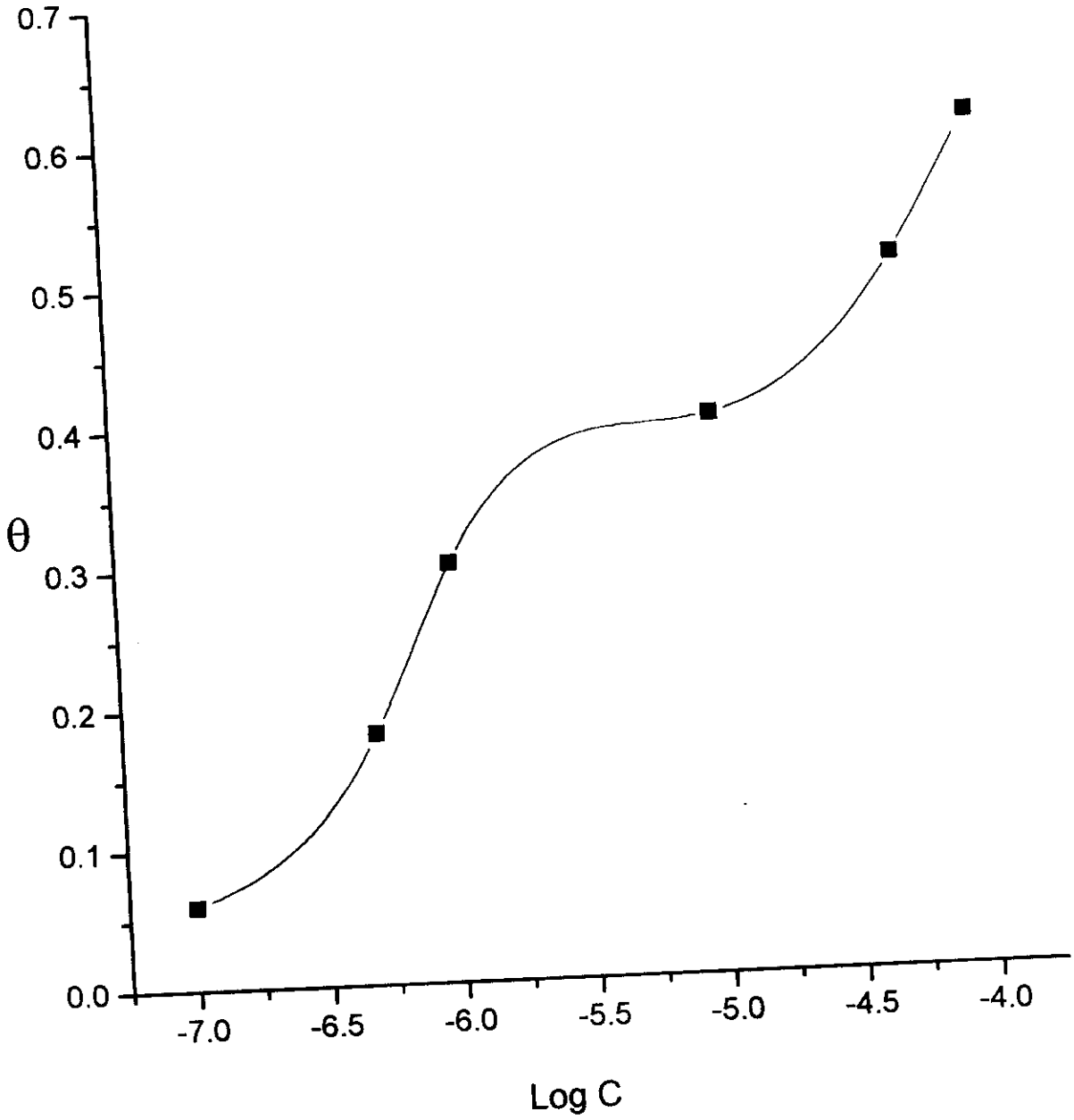

Fig. (3.13): Dependence of θ on the logarithm of inhibitor (I) concentrations

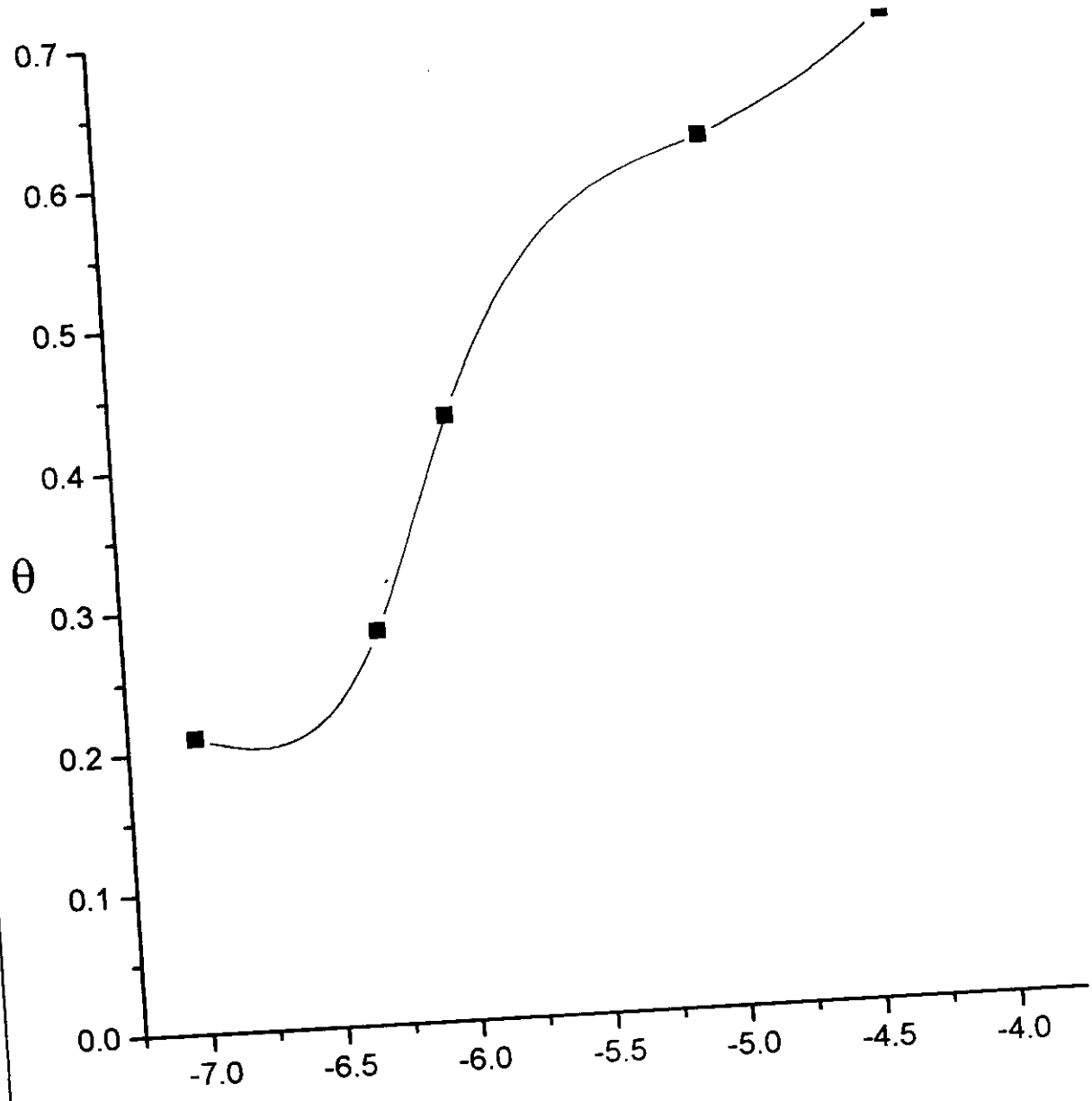

Fig. (3.14): Dependence of θ on the logarithm of inhibitor (II-a) concentrations

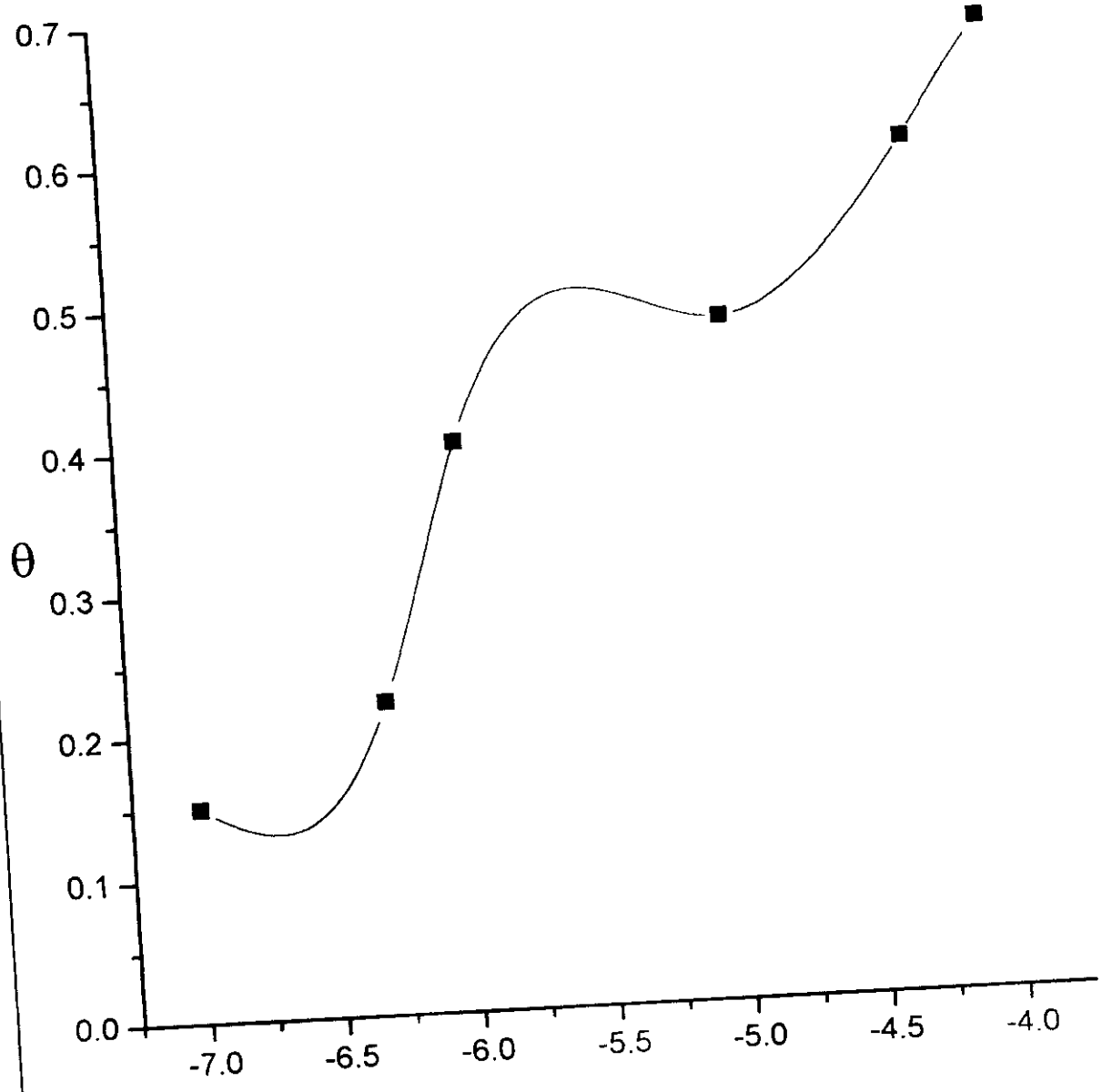

Fig. (3.15): Dependence of θ on the logarithm of inhibitor (II-b) concentrations

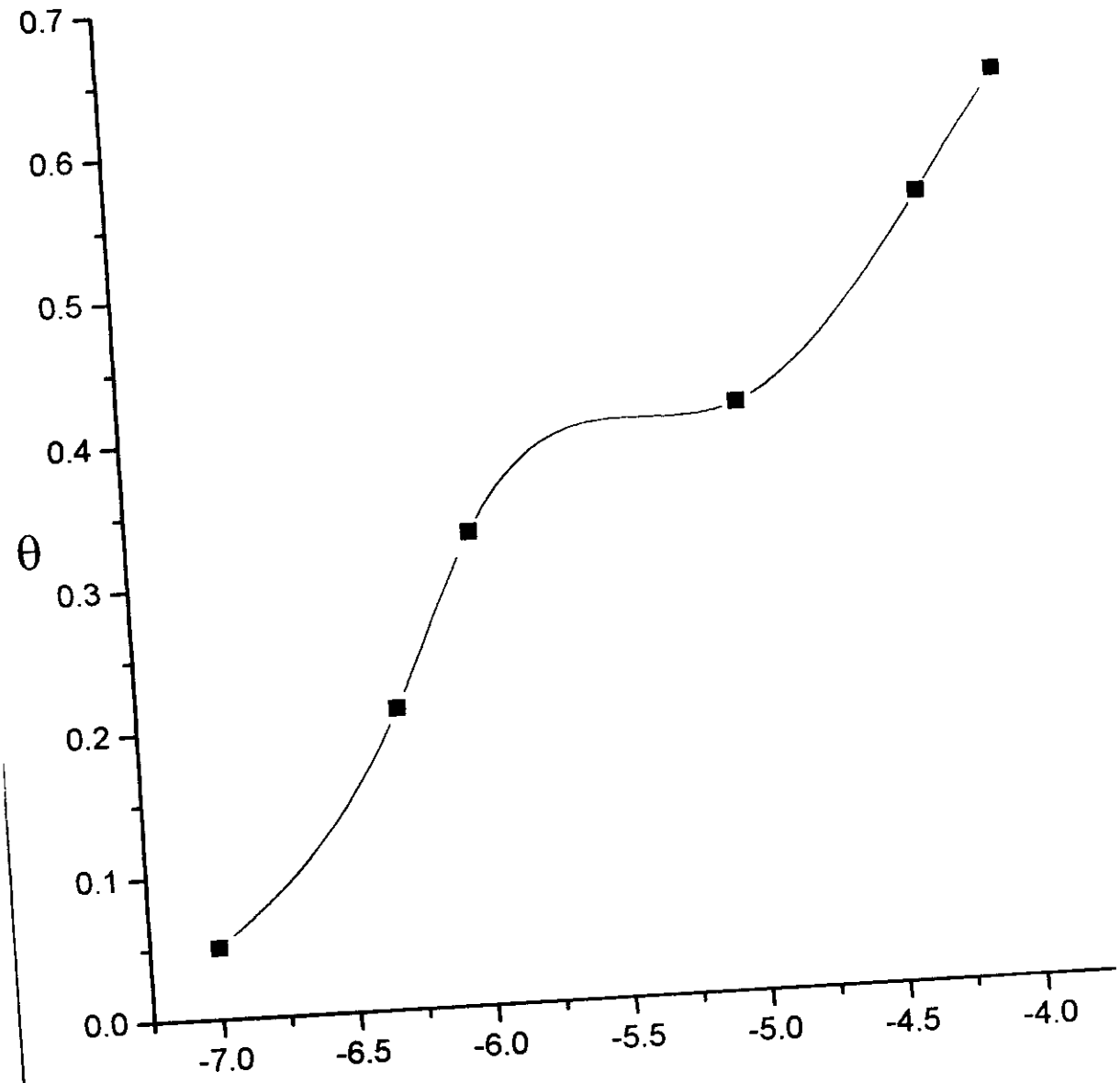

Fig. (3.16): Dependence of θ on the logarithm of inhibitor (II-c) concentrations

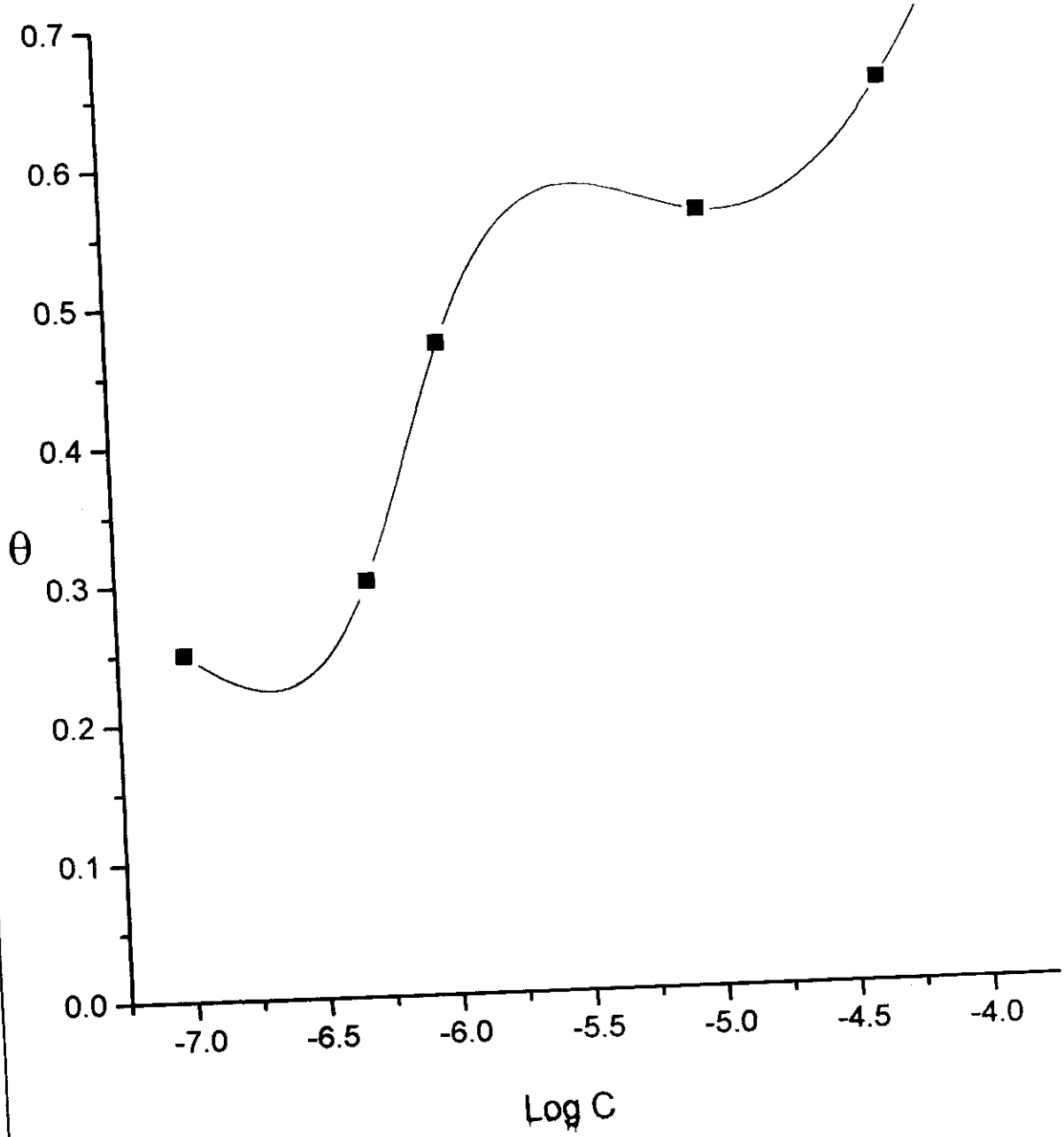

Fig. (3.17): Dependence of θ on the logarithm of inhibitor (III-a) concentrations

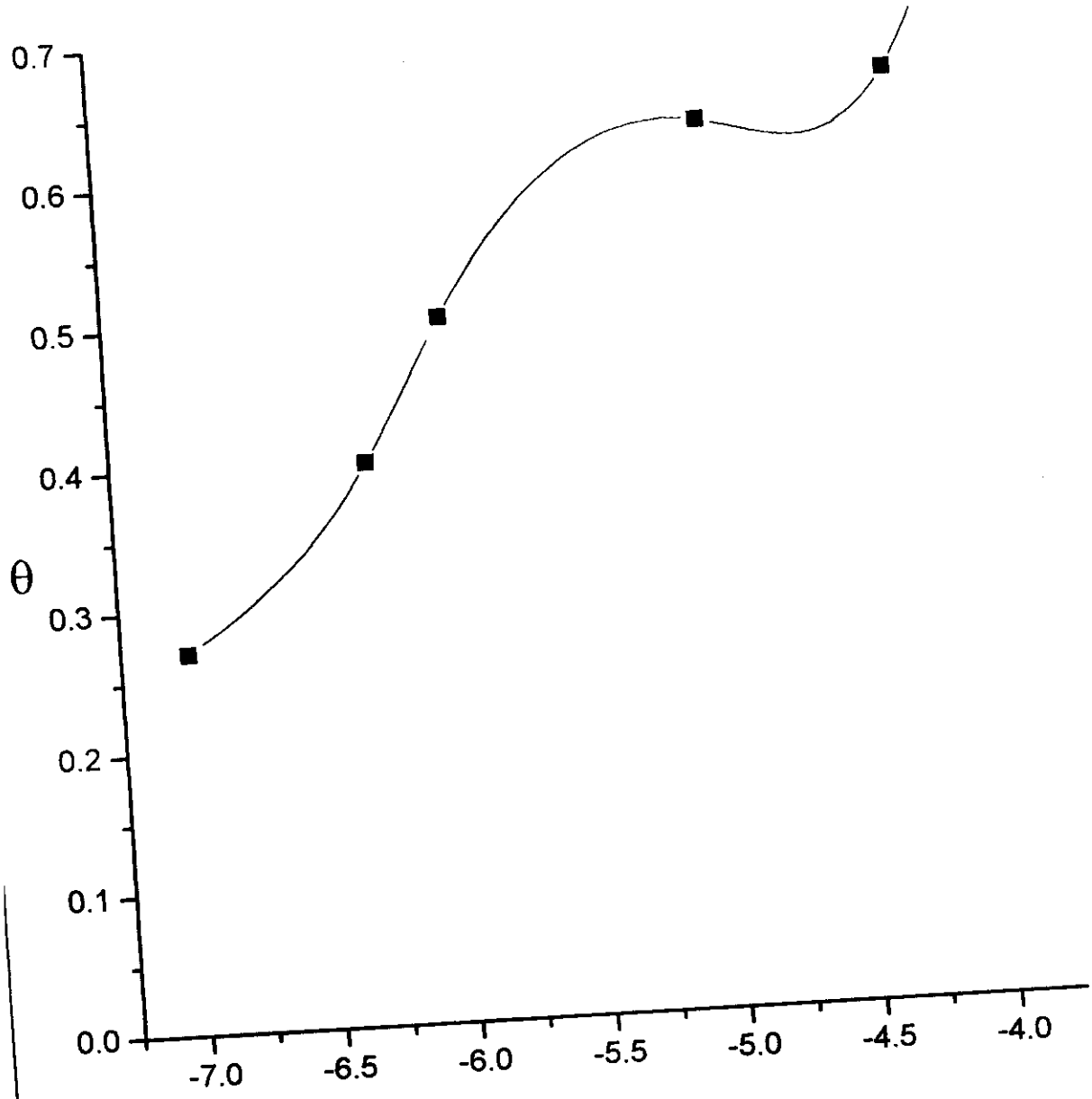

Fig. (3.18): Dependence of θ on the logarithm of inhibitor (III-b) concentrations

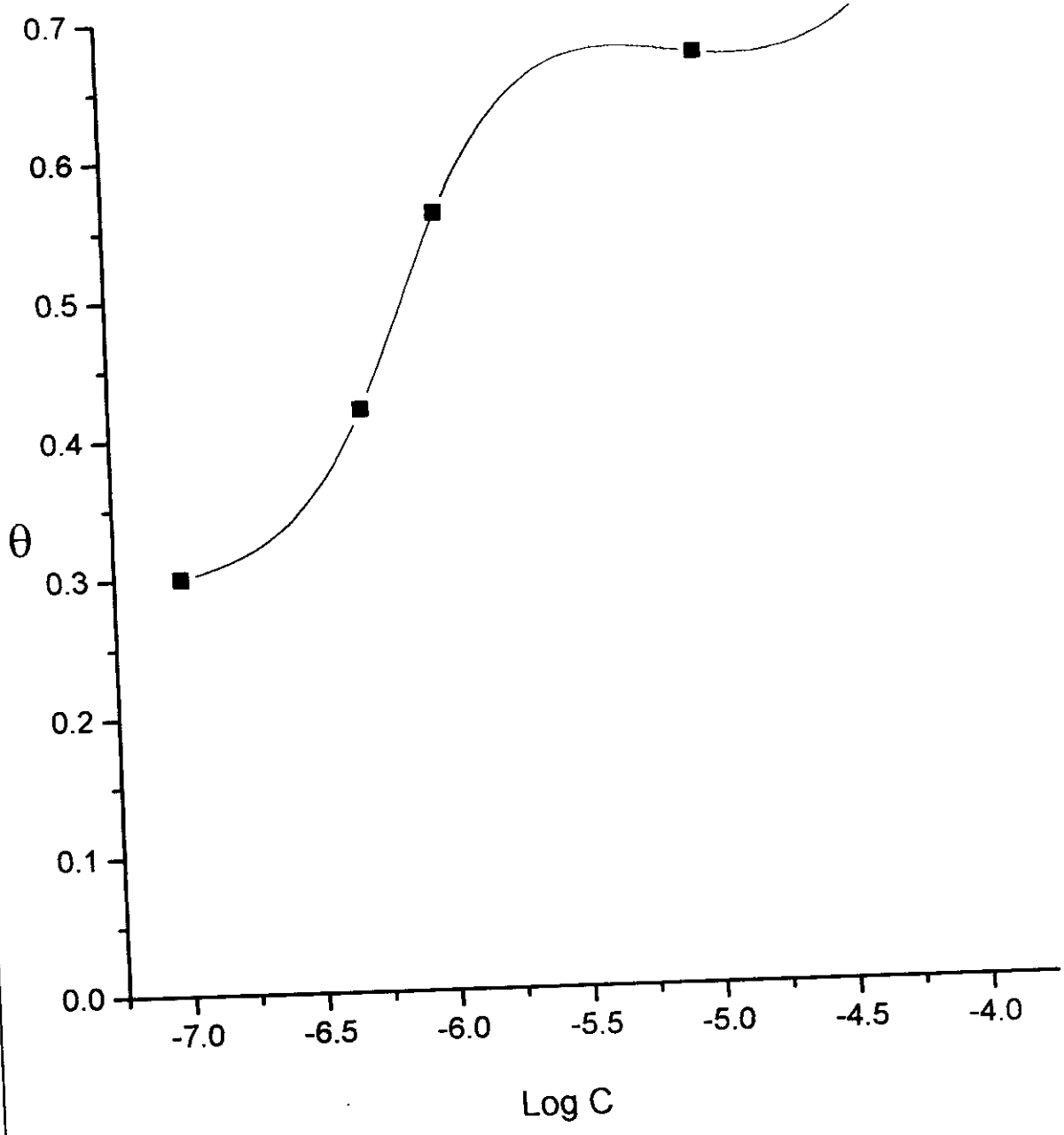

Fig. (3.19): Dependence of θ on the logarithm of inhibitor (III-c) concentrations

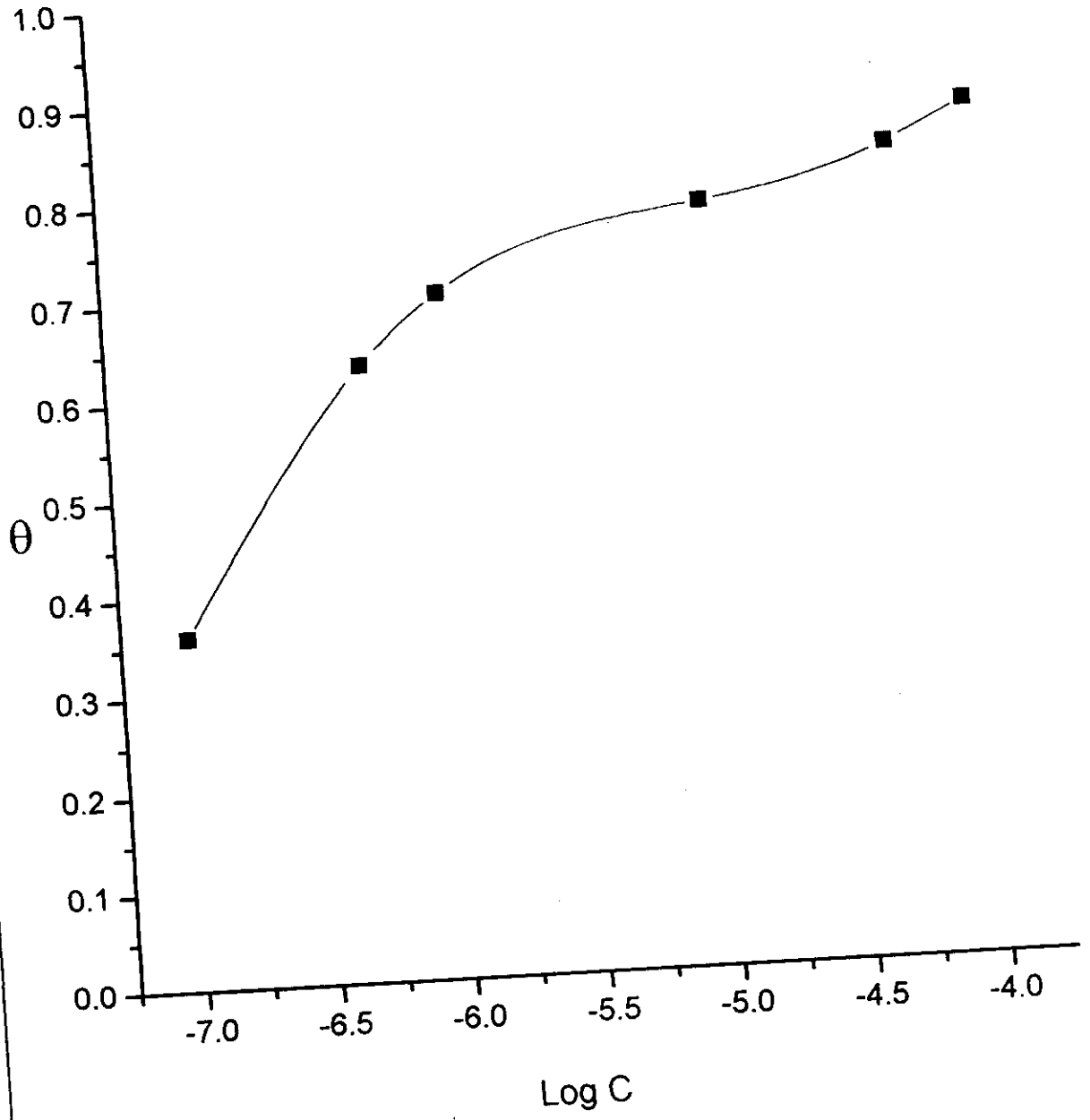

Fig. (3.20): Dependence of θ on the logarithm of inhibitor (IV-a) concentrations

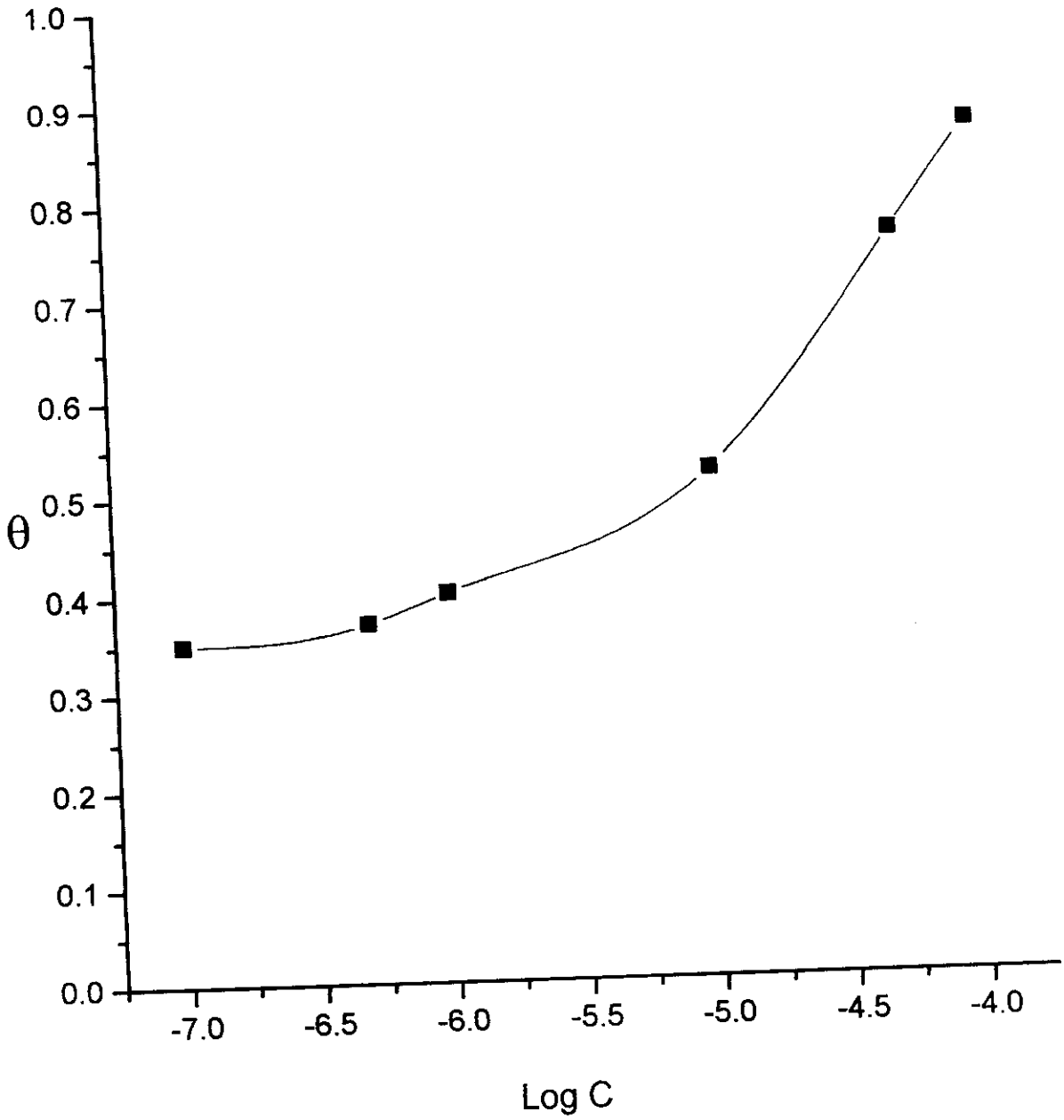

Fig. (3.21): Dependence of θ on the logarithm of inhibitor (IV-b) concentrations

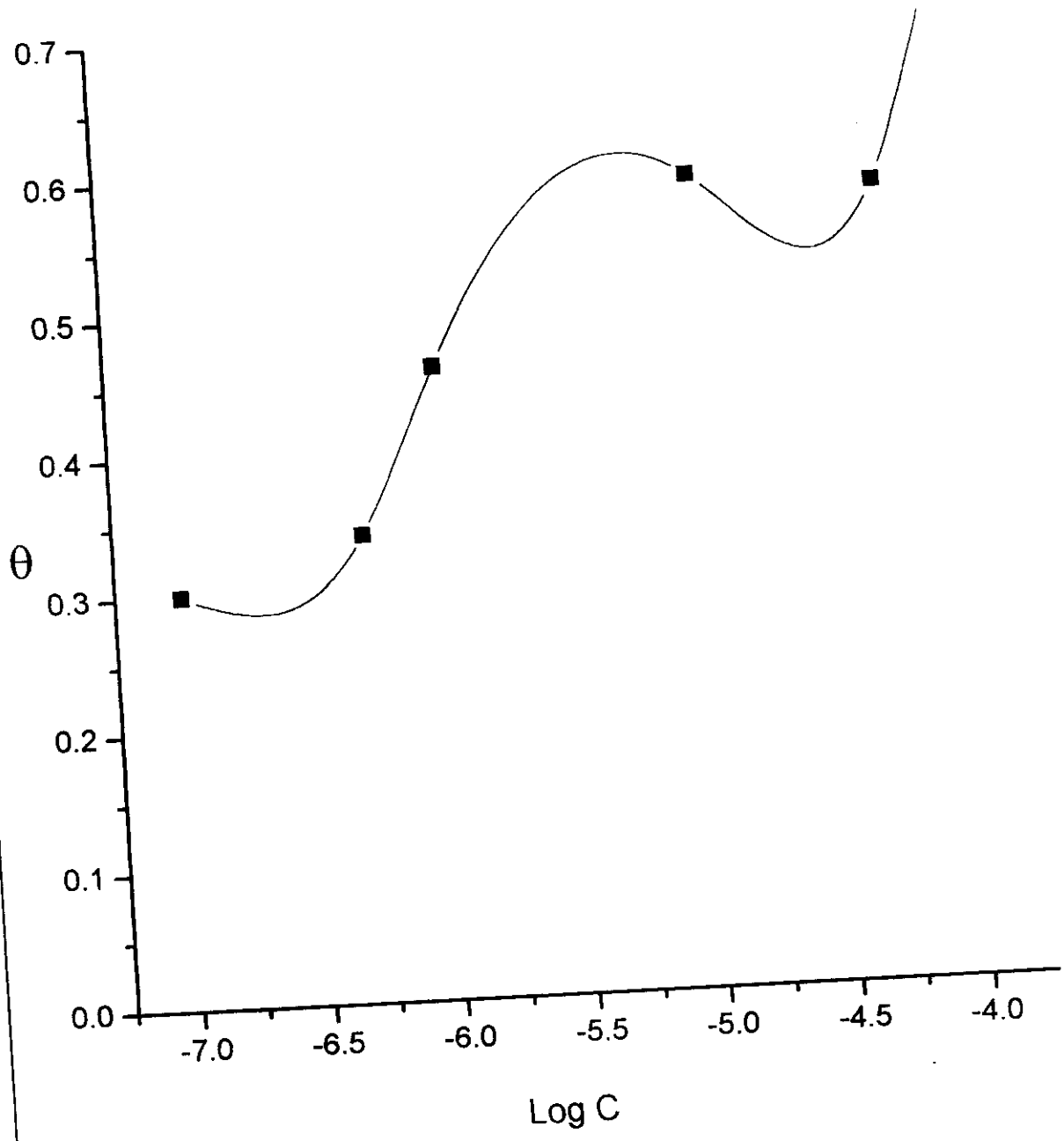

Fig. (3.22): Dependence of θ on the logarithm of inhibitor (IV-c) concentrations

Table(3.1)Data from galvanostatic polarization of carbon steel in 1M HCl containing various concentrations of inhibitor (I) at 30°C

Inh.Conc. (M)	E corr. mv.	I corr. mA cm^{-2}	βc mv dec^{-1}	βa mv dec^{-1}	θi polari.	θ wt. Loss	% Inh.
0. 0	-483	2. 60	215	195	-		-
1 x 10^{-7}	-448	2.29	273	148	0.119	0.100	6.4
5 x 10^{-7}	-440	2.06	250	143	0.207	0.210	18.0
1 x 10^{-6}	-440	1.86	250	137	0.289	0.300	30.0
5 x 10^{-6}	-440	1.69	250	138	0.365	0.370	40.0
1 x 10^{-5}	-440	1.54	250	143	0.407	0.430	50.0
5 x 10^{-5}	-440	1.41	235	138	0.457	0.500	61.0
1x 10^{-4}	-460	1.38	235	166	0.469	0.540	63.0

Table(3. 2)Data from galvanostatic polarization of carbon steel in 1M HCl containing various concentrations of inhibitor (II-a) at 30°C

Inh.Conc. (M)	E corr. mv.	I corr. mA cm^{-2}	βc mv dec^{-1}	βa mv dec^{-1}	θi polari.	θ wt. Loss	% Inh.
0 . 0	-528	2. 80	280	280	-		-
1 x 10^{-7}	-502	2.51	280	228	0.103	0.200	5.0
5 x 10^{-7}	-520	2.13	288	235	0.230	0.240	21.4
1 x 10^{-6}	-487	1.86	296	200	0.325	0.470	33.0
5 x 10^{-6}	-480	1.75	282	200	0.375	0.510	41.0
1 x 10^{-5}	-515	1.54	280	210	0.450	0.550	55.0
5 x 10^{-5}	-486	1.42	280	200	0.500	0.600	63.0
1x 10^{-4}	-480	1.39	280	222	0.503	0.610	65.0

Table(3.3)Data from galvanostatic polarization of carbon steel in 1M HCl containing various concentrations of compound (II-b) at 30°C

Inh.Conc. (M)	E corr. mv.	I corr. mA cm^{-2}	βc mv dec^{-1}	βa mv dec^{-1}	θi polari.	θ wt. Loss	% Inh.
0 . 0	-484	3. 00	307	189		-	-
1 x 10^{-7}	-486	2. 60	307	198	0.150	0.320	15.0
5 x 10^{-7}	-480	2.34	285	181	0.220	0.430	22.0
1 x 10^{-6}	-456	1.88	314	145	0.400	0.490	40.0
5 x 10^{-6}	-466	1.78	266	154	0.480	0.530	48.0
1 x 10^{-5}	-484	1.54	257	160	0.600	0.570	60.0
5 x 10^{-5}	-496	1.41	252	171	0.680	0.650	68.0
1x 10^{-4}	-480	1.38	250	160	0.700	0.700	70.0

Table(3.4)Data from galvanostatic polarization of carbon steel in 1M HCl containing various concentrations of compound (II-c) at 30°C

Inh.Conc. (M)	E corr. mv.	I corr. mA cm^{-2}	βc mv dec^{-1}	βa mv dec^{-1}	θi polari.	θ wt. Loss	% Inh.
0 . 0	-554	4. 60	260	140		-	-
1 x 10^{-7}	-488	3. 30	280	181	0.266	0.340	21.0
5 x 10^{-7}	-516	2.95	285	186	0.301	0.490	28.0
1 x 10^{-6}	-514	2. 30	266	173	0.331	0.530	43.0
5 x 10^{-6}	-508	2.08	250	181	0.366	0.570	51.0
1 x 10^{-5}	-520	1.77	235	174	0.411	0.600	62.0
5 x 10^{-5}	-516	1.68	210	167	0.441	0.700	70.0
1x 10^{-4}	-490	1. 40	222	148	0.533	0.750	75.0

Table(3.5) Data from galvanostatic polarization of carbon steel in 1M HCl containing various concentrations of inhibitor (III-a) at 30°C

Inh.Conc. (M)	E corr. mv.	I corr. mA cm^{-2}	βc mv dec^{-1}	βa mv dec^{-1}	θi polari.	θ wt. Loss	% Inh.
0 . 0	-500	3. 00	215	207	-		-
1 x 10^{-7}	-512	2. 20	200	212	0.266	0.310	25.0
5 x 10^{-7}	-500	2. 10	200	200	0.300	0.450	30.0
1 x 10^{-6}	-492	1. 60	250	200	0.466	0.520	47.0
5 x 10^{-6}	-488	1. 40	250	200	0.533	0.550	56.0
1 x 10^{-5}	-500	1.32	280	200	0.560	0.600	65.0
5 x 10^{-5}	-488	1.11	240	200	0.630	0.700	75.0
1x 10^{-4}	-488	1.05	285	200	0.666	0.730	80.0

Table(3.6)Data from galvanostatic polarization of carbon steel in 1M HCl containing various concentrations of inhibitor (III-b) at 30°C

Inh.Conc. (M)	E corr. mv.	I corr. mA cm^{-2}	βc mv dec^{-1}	βa mv dec^{-1}	θi polari.	θ wt. Loss	% Inh.
0 . 0	-544	3. 00	278	285	-	-	-
1 x 10^{-7}	-540	2. 40	235	266	0.220	0.230	27.0
5 x 10^{-7}	-520	2. 10	260	230	0.300	0.420	40.0
1 x 10^{-6}	-528	1. 80	222	226	0.400	0.490	50.0
5 x 10^{-6}	-512	1. 50	266	200	0.500	0.520	63.0
1 x 10^{-5}	-504	1.41	248	208	0.530	0.550	66.0
5 x 10^{-5}	-496	1.21	233	182	0.580	0.660	78.0
1x 10^{-4}	-492	1.11	260	180	0.630	0.700	82.0

Table(3.7)Data from galvanostatic polarization of carbon steel in 1M HCl containing various concentrations of Inhibitor (III-c) at 30°C

Inh.Conc. (M)	E corr. mv.	I corr. mA cm^{-2}	βc mv dec^{-1}	βa mv dec^{-1}	θi polari.	θ wt. Loss	% Inh.
0 . 0	-532	3. 00	213	285		-	-
1 x 10^{-7}	-542	2. 20	250	240	0.266	0.230	30.0
5 x 10^{-7}	-524	2.01	260	223	0.333	0.380	42.0
1 x 10^{-6}	-536	1.61	224	220	0.466	0.500	56.0
5 x 10^{-6}	-512	1.42	240	200	0.533	0.510	67.0
1 x 10^{-5}	-504	1.21	240	200	0.596	0.540	72.0
5 x 10^{-5}	-496	1.12	275	167	0.633	0.640	80.0
1x 10^{-4}	-492	1.01	240	172	0.660	0.680	84.0

Table(3.8)Data from galvanostatic polarization of carbon steel in 1M HCl containing various concentrations of inhibitor (IV-a) at 30°C

Inh.Conc. (M)	E corr. mv.	I corr. mA cm^{-2}	βc mv dec^{-1}	βa mv dec^{-1}	θi polari.	θ wt. Loss	% Inh.
0 . 0	-512	2.75	266	147	-		-
1 x 10^{-7}	-488	2.04	260	160	0.300	0.370	30.0
5 x 10^{-7}	-524	1.86	240	189	0.340	0.540	34.0
1 x 10^{-6}	-496	1.65	245	174	0.460	0.580	46.0
5 x 10^{-6}	-520	1.47	225	176	0.590	0.600	59.0
1 x 10^{-5}	-532	1.34	214	183	0.680	0.670	68.0
5 x 10^{-5}	-476	1.25	250	134	0.760	0.740	76.0
1x 10^{-4}	-496	1.12	235	160	0.880	0.770	88.0

Table (3. 9) Data from galvanostatic polarization of carbon steel in 1M HCl containing various concentrations of inhibitor(IV-b) at 30 C

Inh.Conc. (M)	E corr. mv.	I corr. mA cm^{-2}	βc mv dec^{-1}	βa mv dec^{-1}	θi polari.	θ wt. Loss	% Inh.
0 . 0	-514	2.85	250	174	-		-
1 x 10^{-7}	-546	2.18	200	190	0.250	0.550	25.0
5 x 10^{-7}	-514	1.92	220	176	0.370	0.490	37.0
1 x 10^{-6}	-494	1.86	250	154	0.400	0.540	40.0
5 x 10^{-6}	-516	1.64	226	171	0.520	0.630	52.0
1 x 10^{-5}	-532	1.28	200	166	0.760	0.700	76.0
5 x 10^{-5}	-510	1.09	215	145	0.870	0.740	87.0
1x 10^{-4}	-514	1.07	210	147	0.930	0.780	93.0

Table (3. 10) Data from galvanostatic polarization of carbon steel in 1M HCl containing various concentrations of inhibitor (IV-c) at 30 C

Inh.Conc. (M)	E corr. mv.	I corr. mA cm^{-2}	βc mv dec^{-1}	βa mv dec^{-1}	θi polari.	θ wt. Loss	% Inh.
0 . 0	-528	2.95	280	196	-		-
1 x 10^{-7}	-518	1.99	255	167	0.360	0.380	36.0
5 x 10^{-7}	-515	1.47	240	180	0.630	0.660	63.0
1 x 10^{-6}	-555	1.38	200	160	0.700	0.700	70.0
5 x 10^{-6}	500	1.25	225	156	0.780	0.730	78.0
1 x 10^{-5}	-500	1.2	210	150	0.830	0.760	83.0
5 x 10^{-5}	-492	1.14	218	143	0.870	0.800	87.0
1x 10^{-4}	-495	1.07	250	140	0.940	0.830	94.0

Table (3.11): Inhibition efficiency of all inhibitors at different concentrations as determined by polarization measurements at 303 K

[Inh.],M	% inhibition									
		Para-			Meta-			Ortho-		
	I	II NO_2	III CH_3	IV OCH_3	II NO_2	III CH_3	IV OCH_3	II NO_2	III CH_3	IV OCH_3
$1X10^{-7}$	11.9	10.3	26.6	30	15.5	22	25	25.0	26.6	36
$5X10^{-7}$	20.7	23.0	30.0	34	22.0	30	37	30.1	33.3	63
$1X10^{-6}$	28.9	32.5	46.6	46	40.0	40	40	33.1	46.6	70
$5X10^{-6}$	36.5	37.5	53.3	59	48.0	50	52	36.6	53.3	78
$1X10^{-5}$	40.7	45.0	56.0	68	60.0	53	76	41.1	59.6	83
$5X10^{-5}$	45.7	50.0	63.0	76	68.0	58	87	44.1	63.3	87
$1X01^{-4}$	46.9	50.3	66.6	88	70.0	63	93	53.3	66.0	94

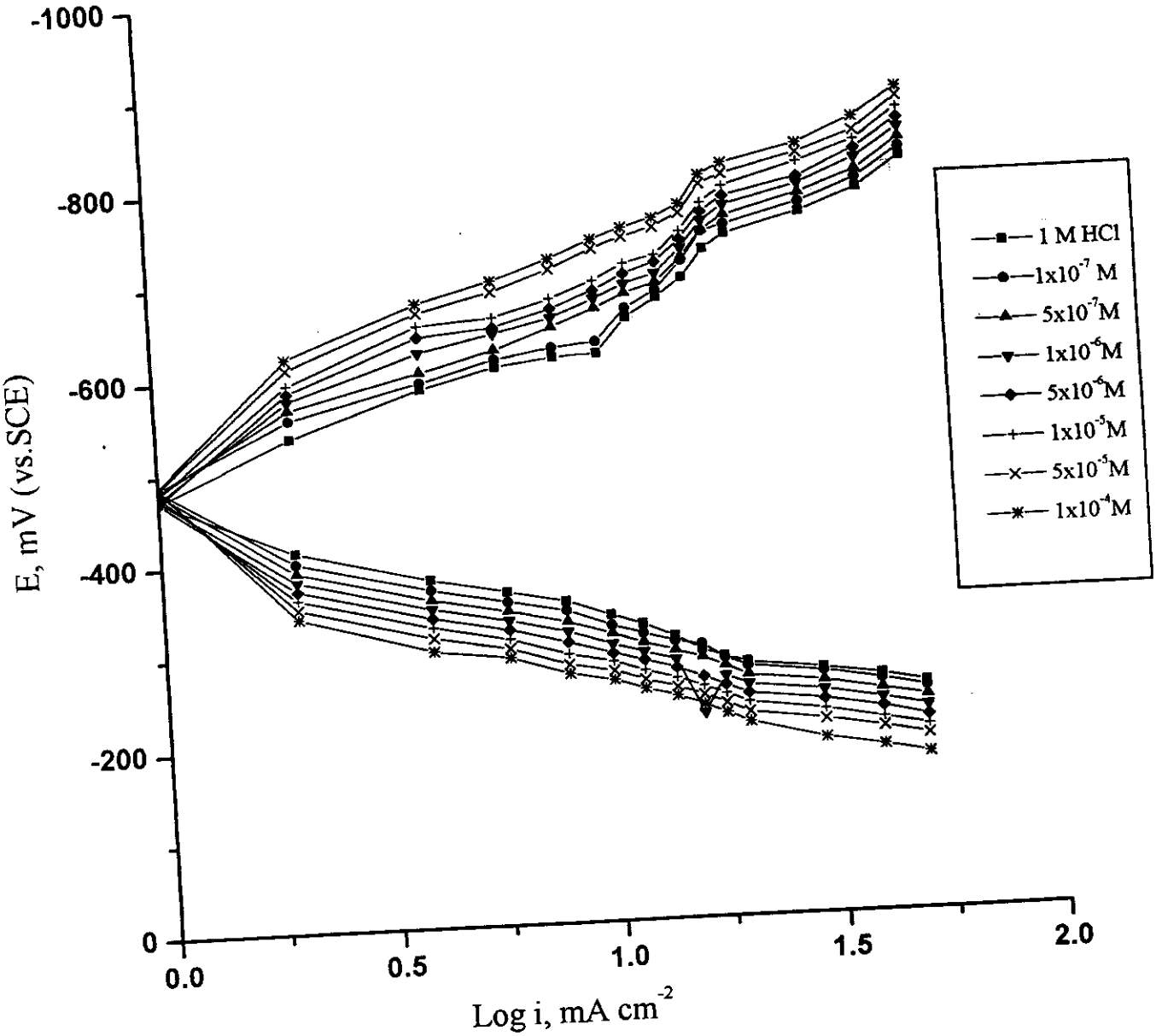

Fig.(3.23): Galvanostatic polarization curves for C-steel in 1 M HCl in the absence and presence of different concentrations of inhibitor (II-a)

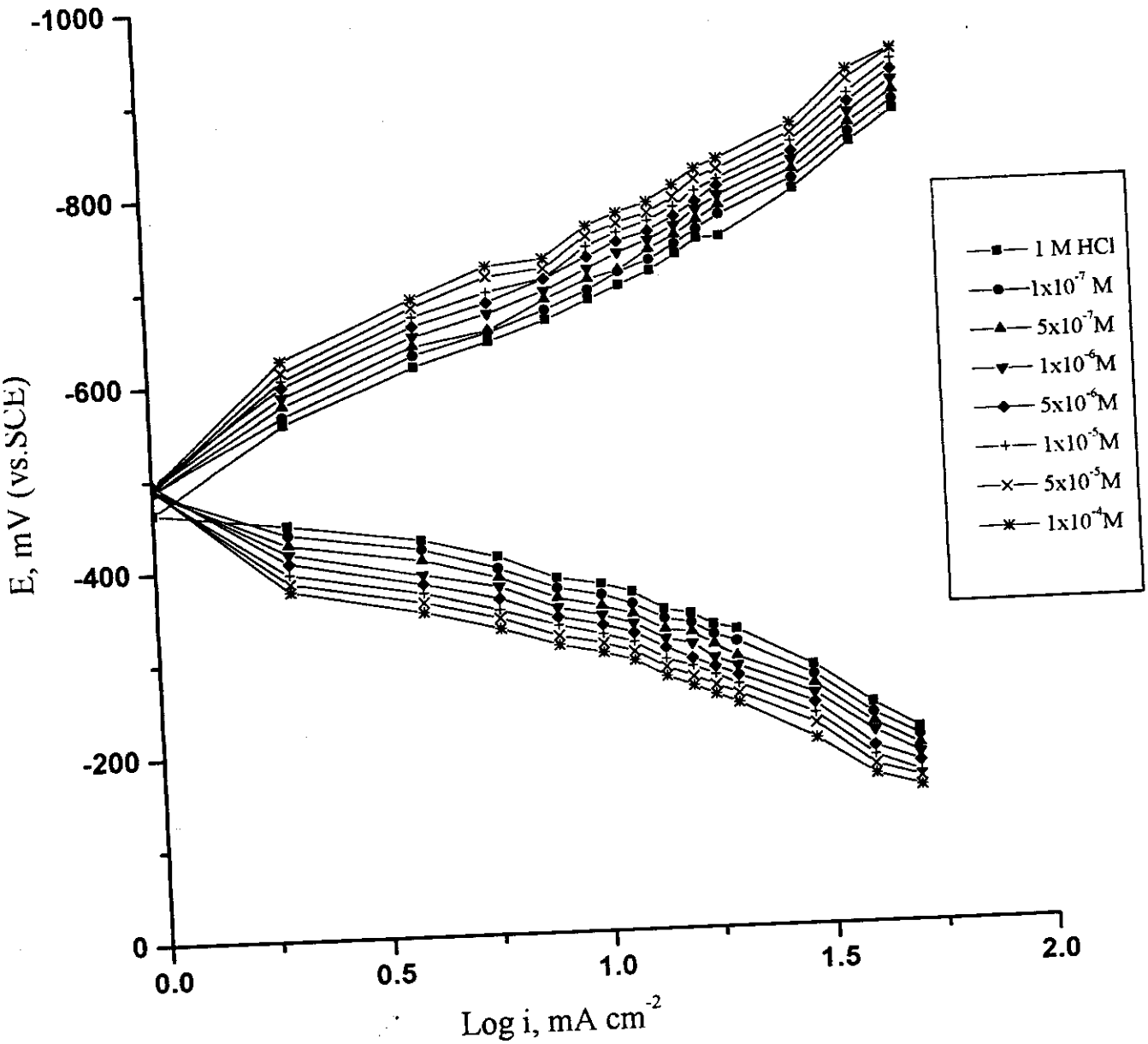

Fig.(3.24): Galvanostatic polarization curves for C-steel in 1 M HCl in the absence and presence of different concentrations of inhibitor (II-b)

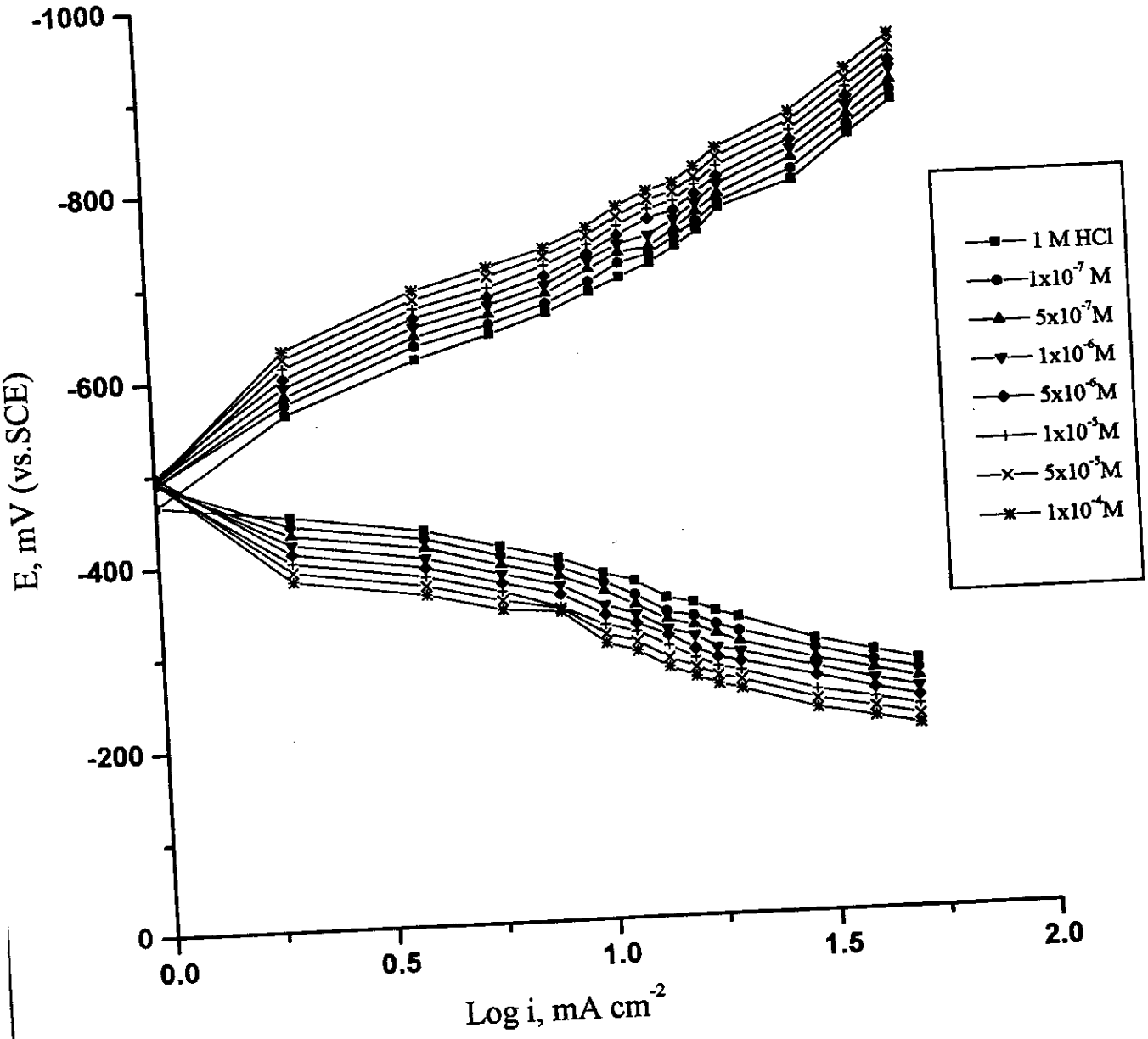

Fig.(3.25): Galvanostatic polarization curves for C-steel in 1 M HCl in the absence and presence of different concentrations of inhibitor (II-c)

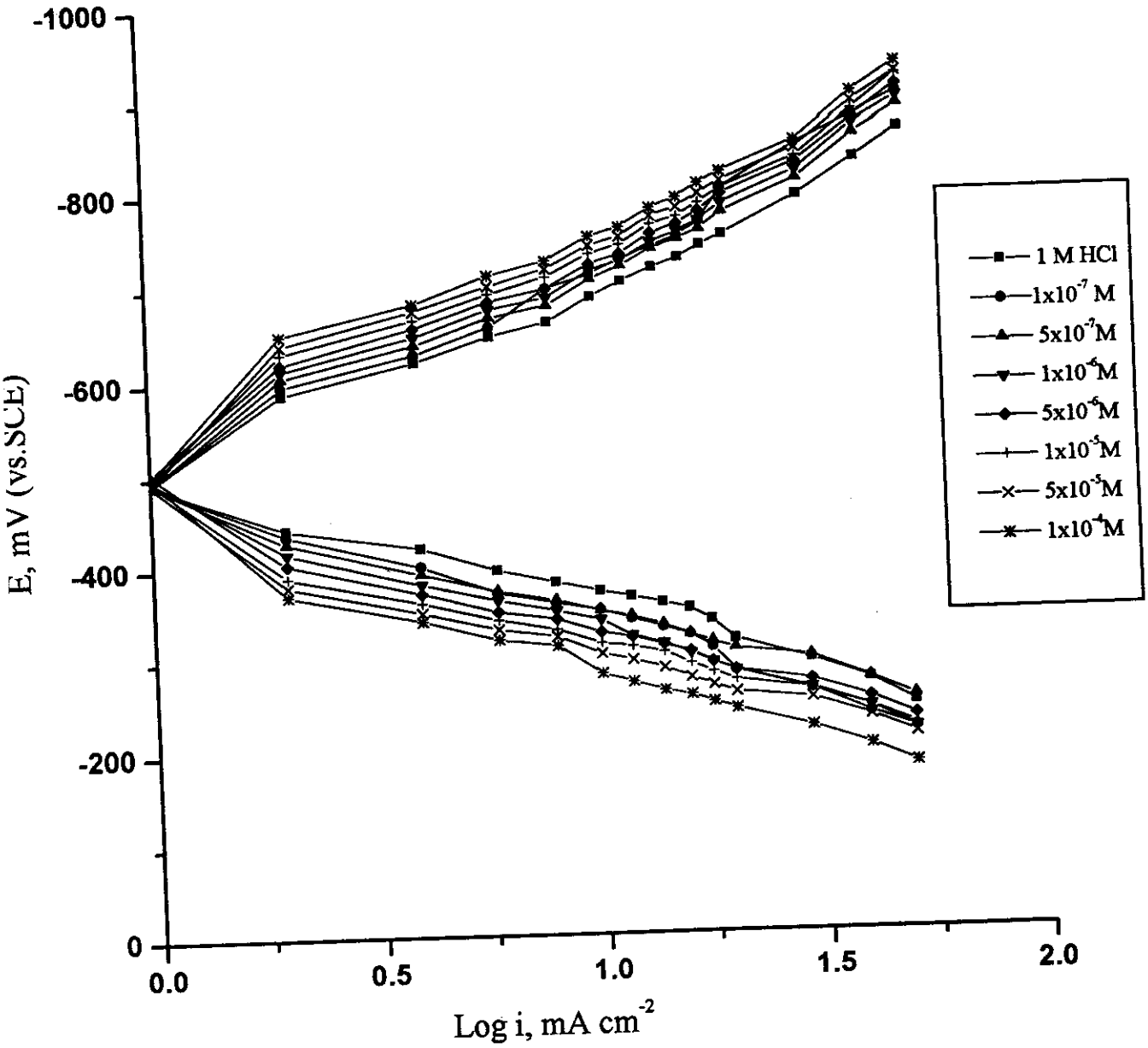

Fig.(3.26): Galvanostatic polarization curves for C-steel in 1 M HCl in the absence and presence of different concentrations of inhibitor (III-a)

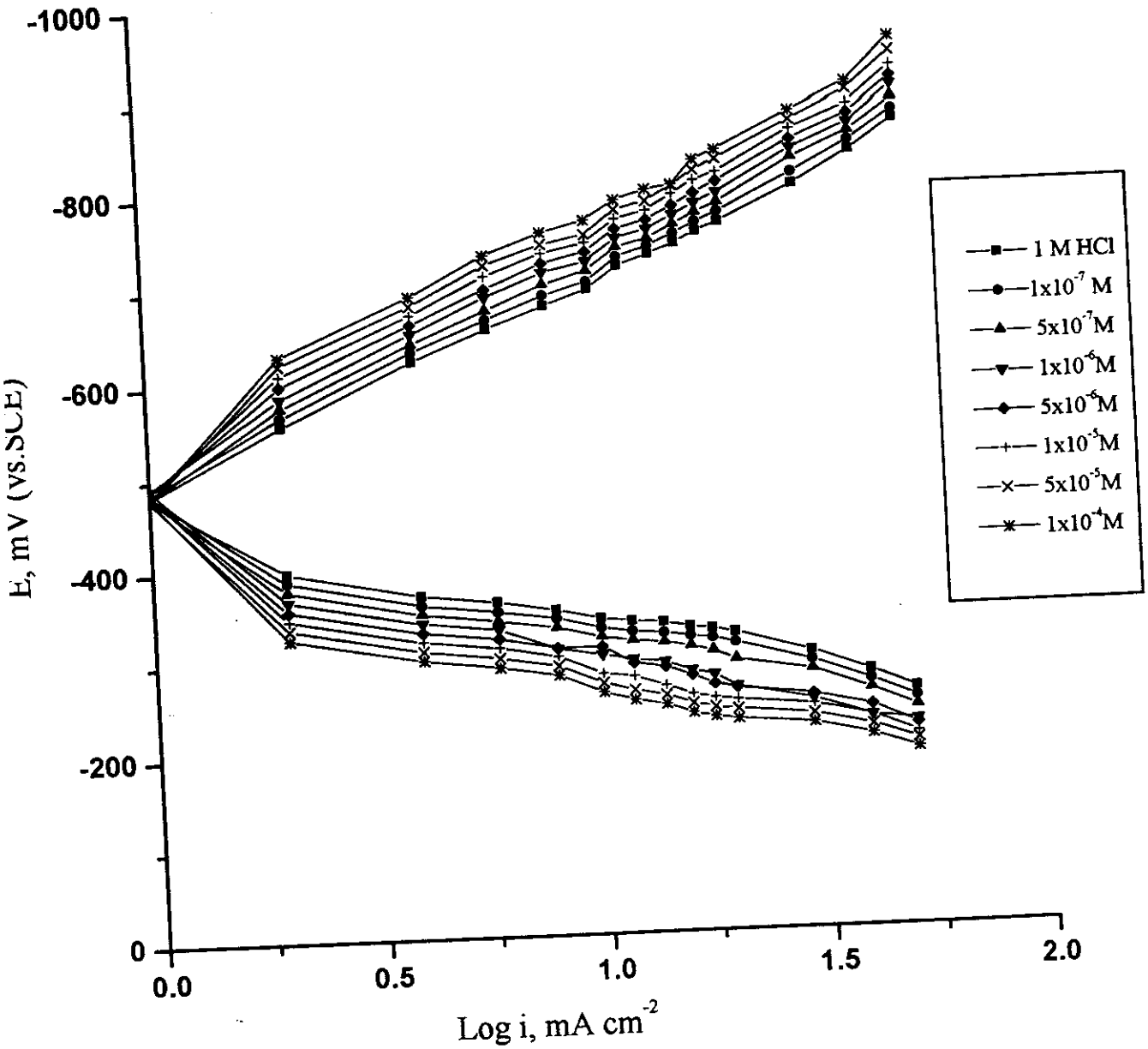

Fig.(3.27): Galvanostatic polarization curves for C-steel in 1 M HCl in the absence and presence of different concentrations of inhibitor (III-b)

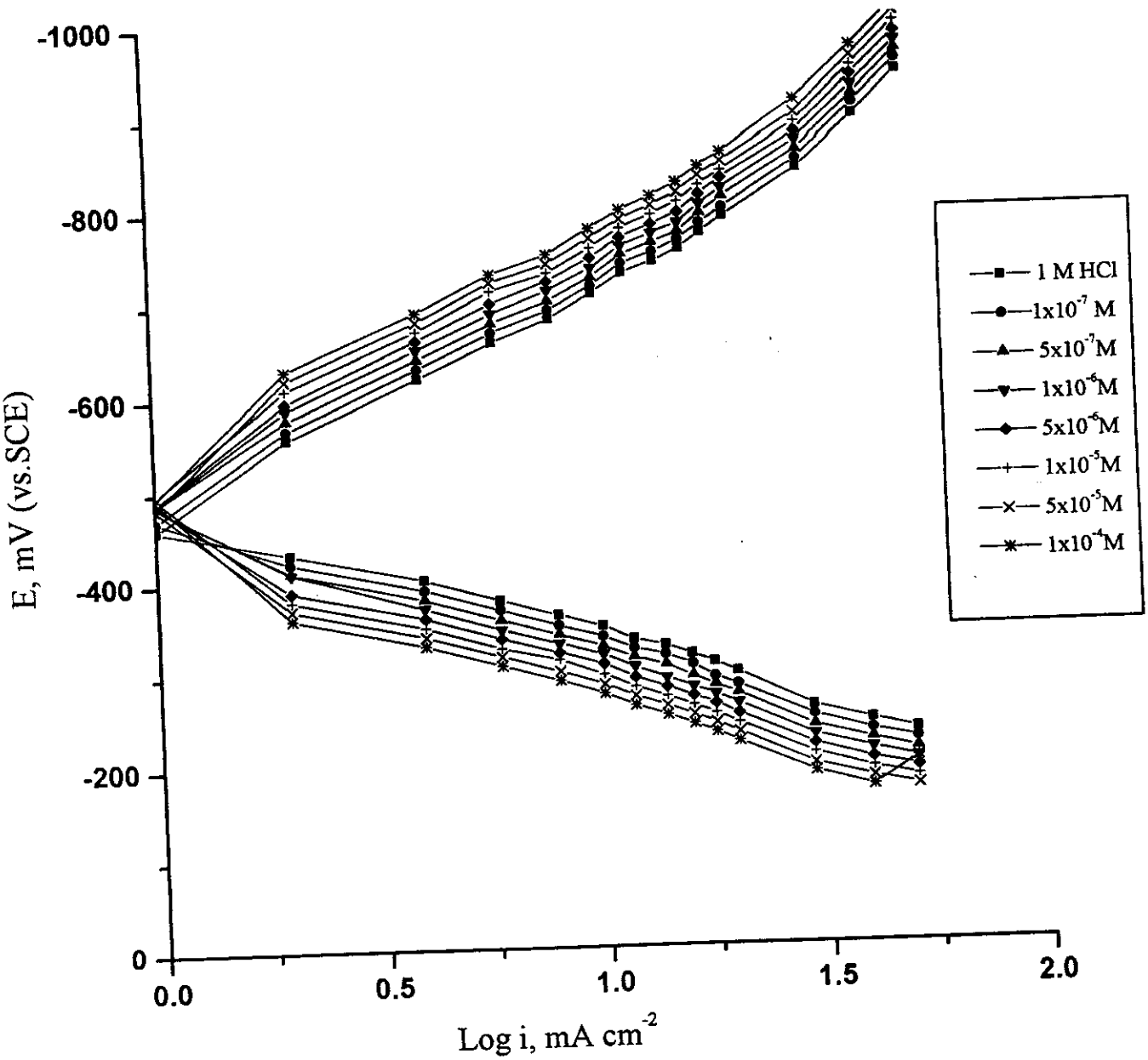

Fig.(3.28): Galvanostatic polarization curves for C-steel in 1 M HCl in the absence and presence of different concentrations of inhibitor (III-c)

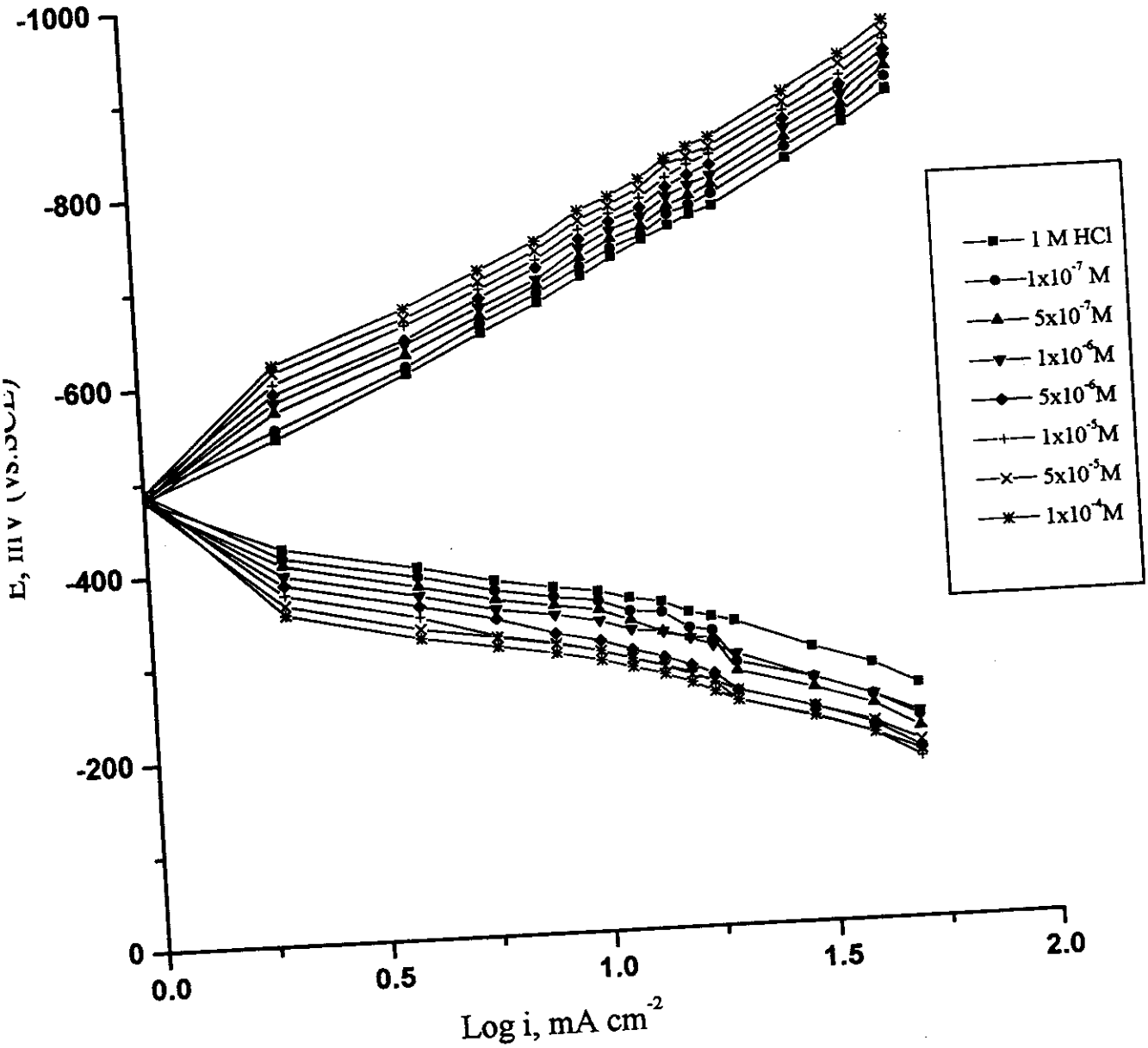

Fig.(3.29): Galvanostatic polarization curves for C-steel in 1 M HCl in the absence and presence of different concentrations of inhibitor (IV-a)

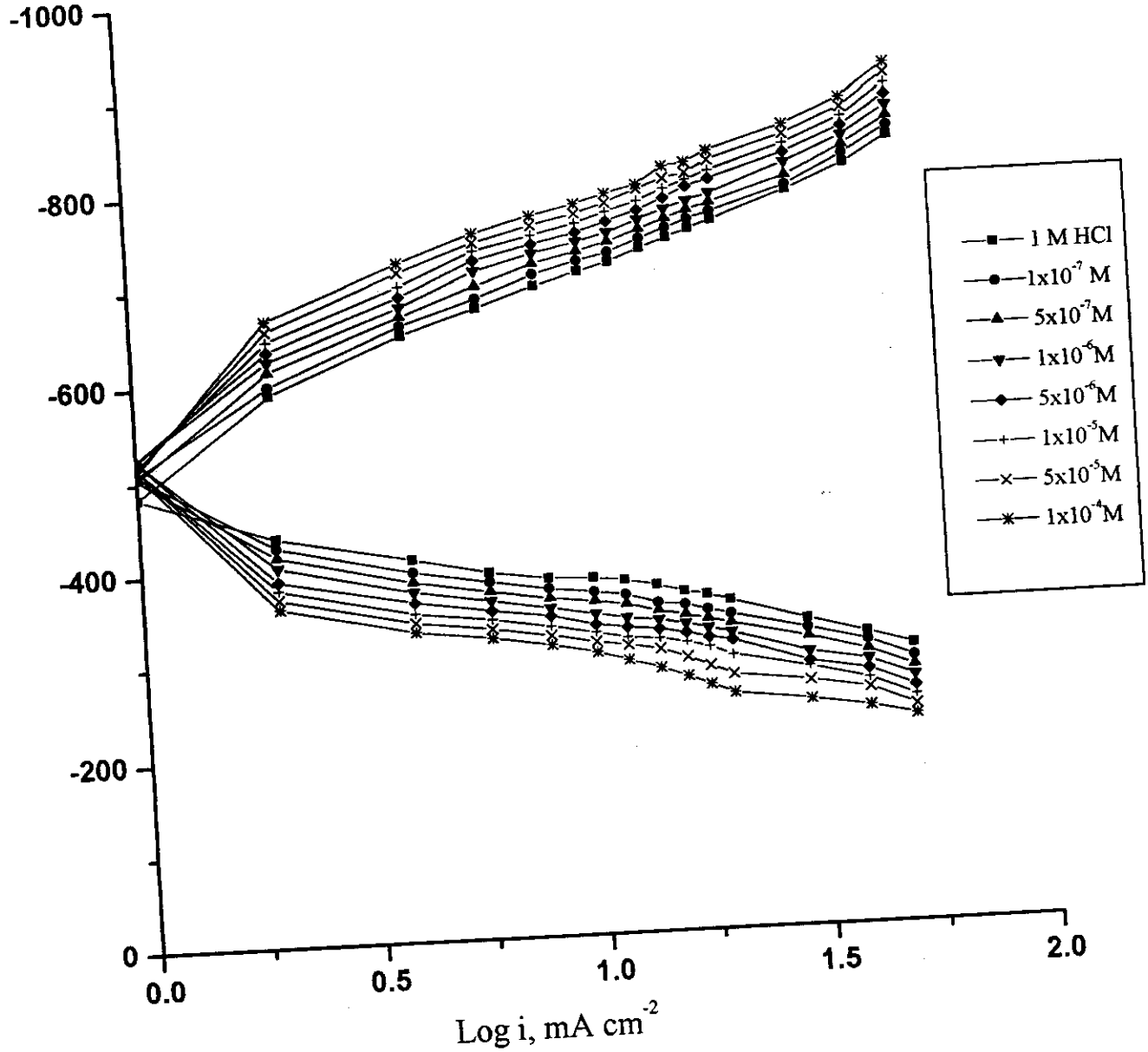

Fig.(3.30): Galvanostatic polarization curves for C-steel in 1 M HCl in the absence and presence of different concentrations of inhibitor (IV-b)

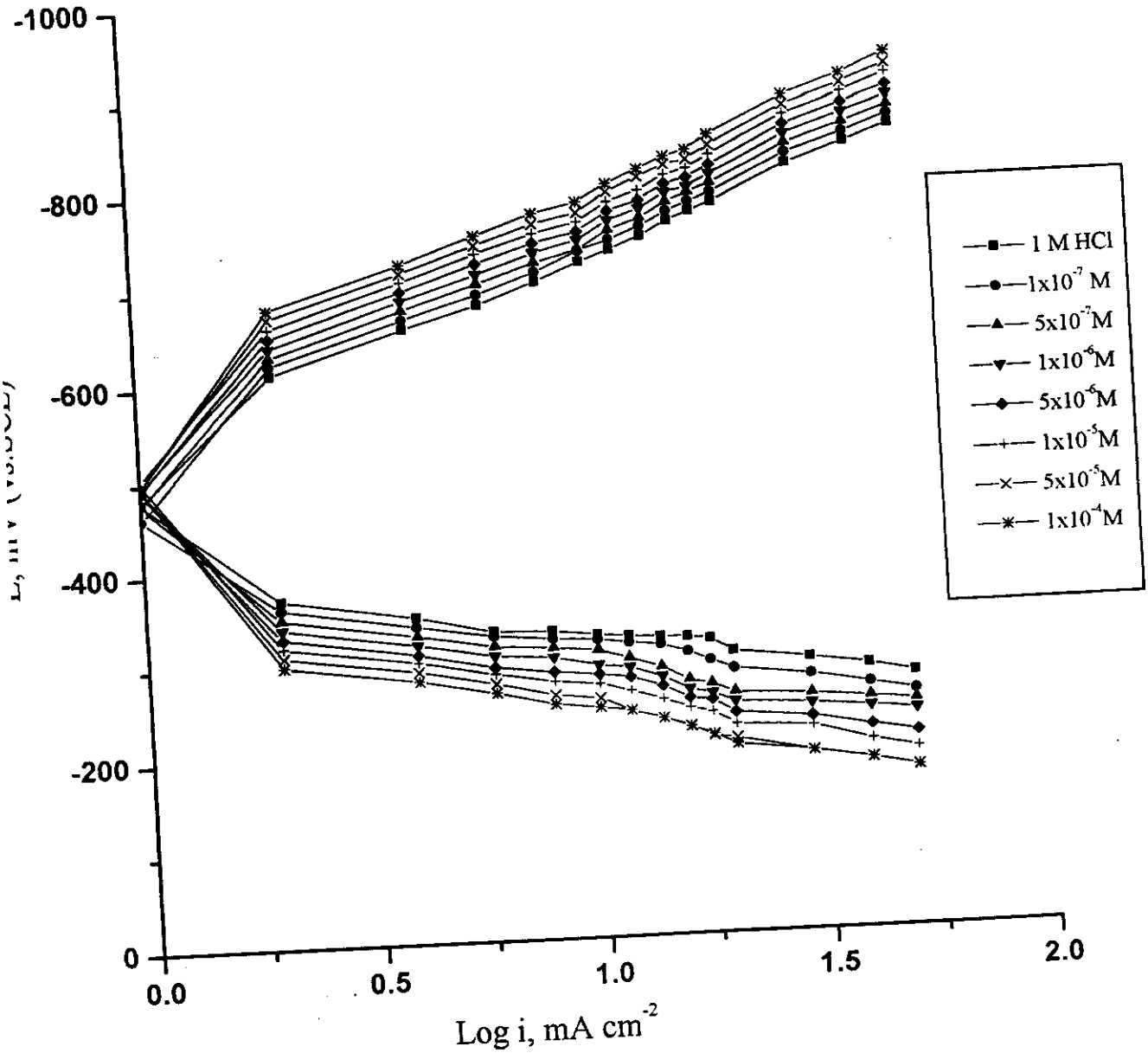

Fig.(3.31): Galvanostatic polarization curves for C-steel in 1 M HCl in the absence and presence of different concentrations of inhibitor (IV-c)

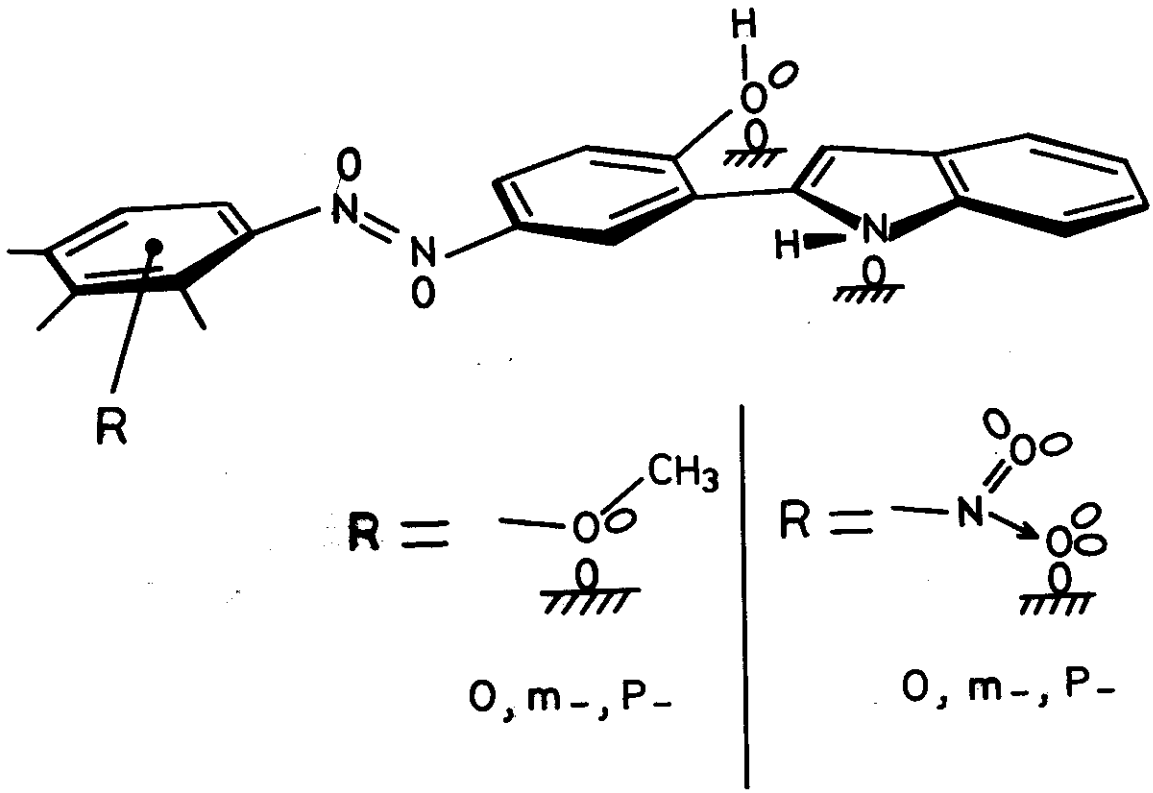

Fig.(3.32) Skeletal repres eutation of compounds (1 - Ⅳ)

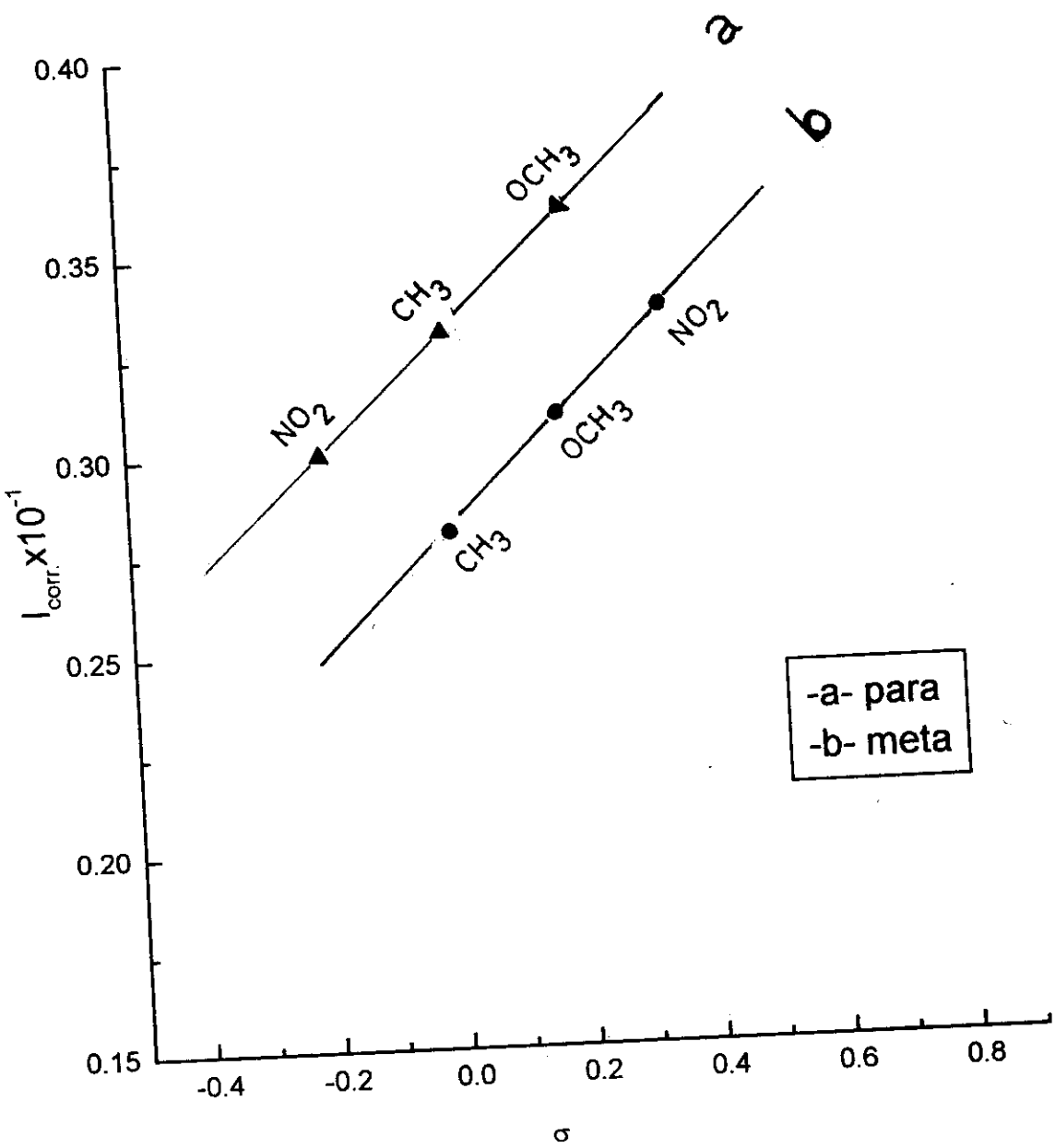

Fig.(3.33) : Variation of corrosion curent $I_{corr.}$,with substituent constant, σ, of the substituent group in (a)para and (b) meta position with respect of the azo group of indole derivatives

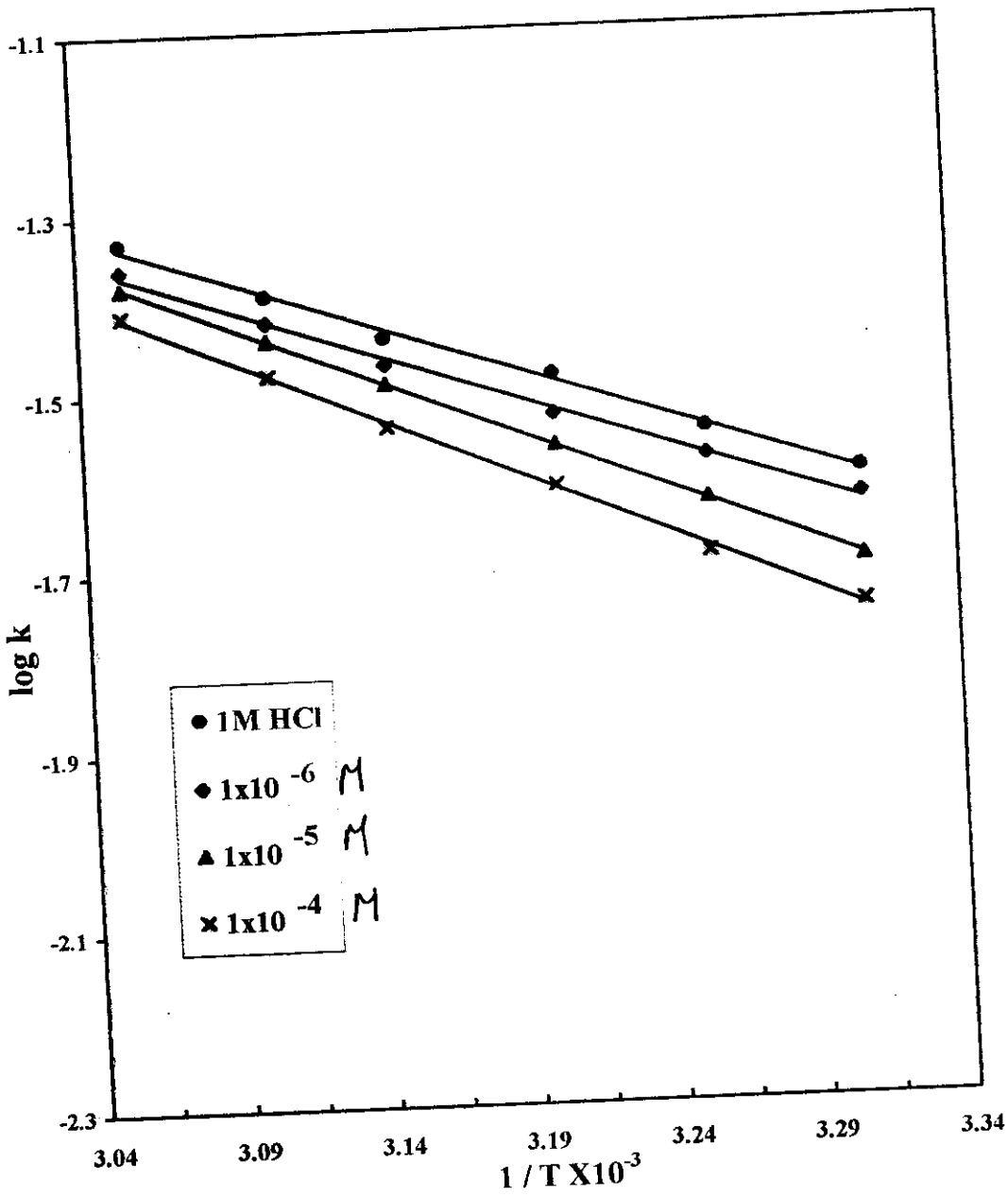

Fig (3.34): log K- 1/T curves for carbon steel dissolution in 1 M HCl in the absence and presence of different concentrations of inhibitor (1)

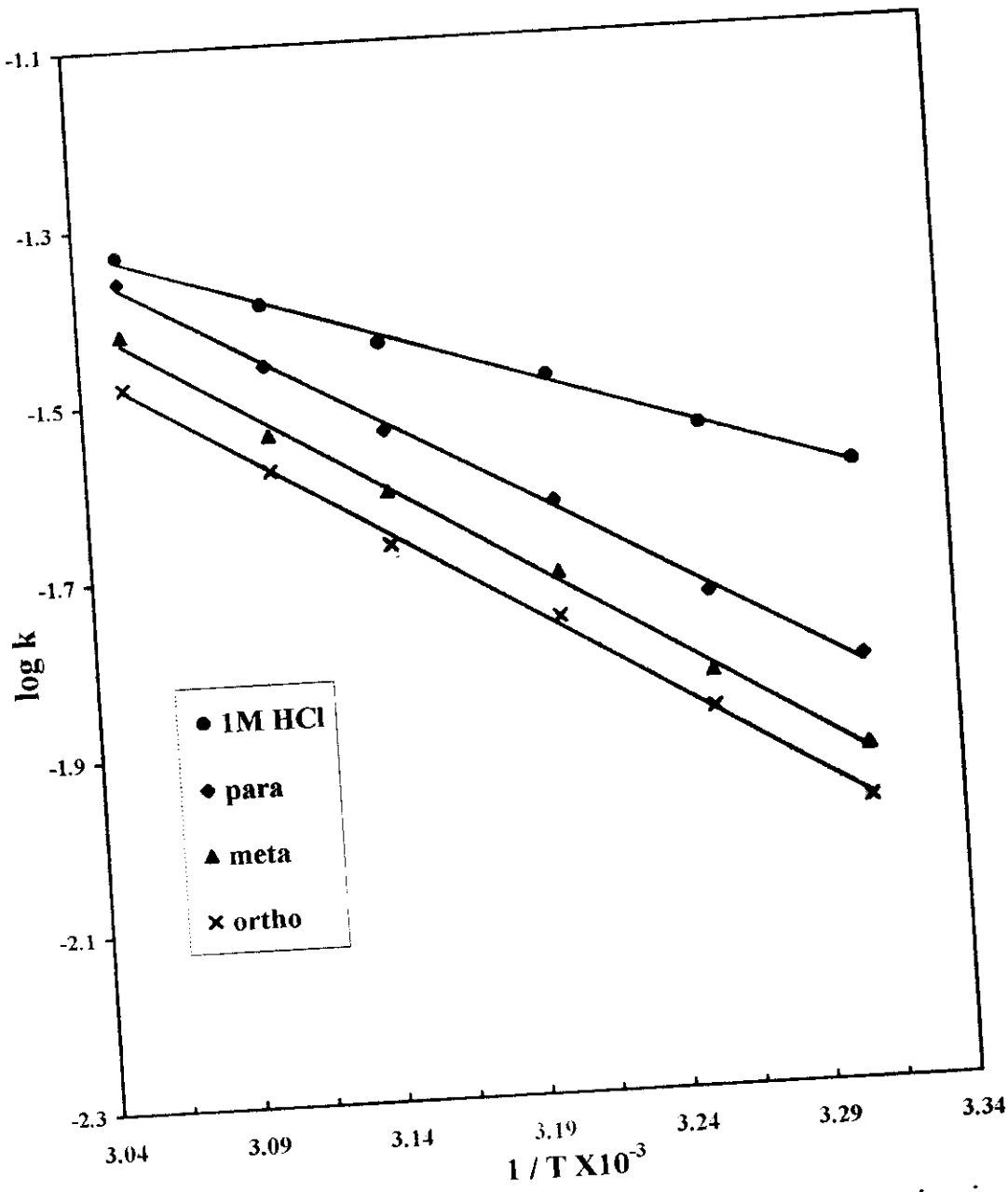

Fig (3.35): log K- 1/T curves for carbon steel dissolution in 1 M HCl in the absence and presence of 10^{-4} M of inhibitor (II-a)

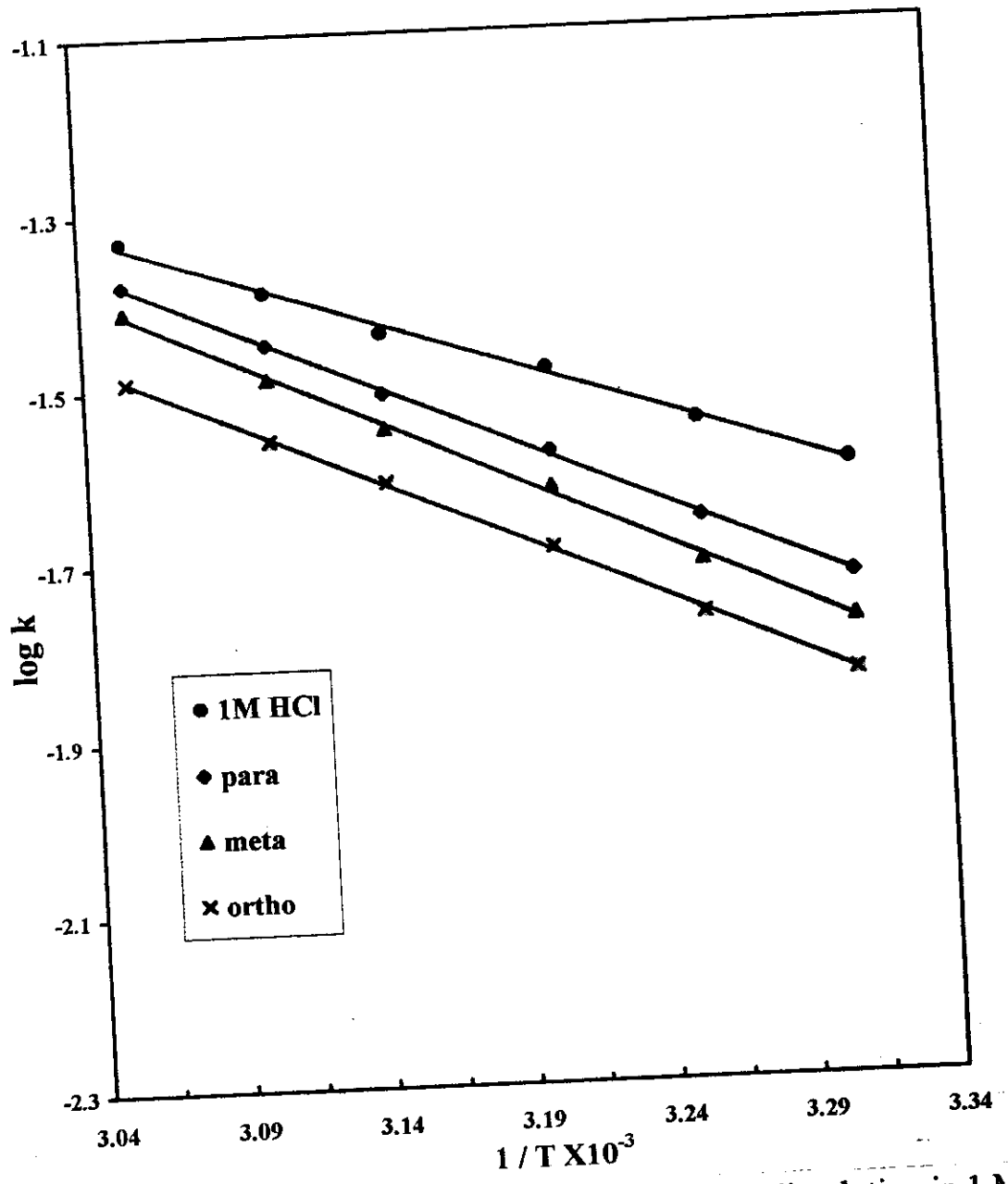

Fig (3.36): log K- 1/T curves for carbon steel dissolution in 1 M HCl in the absence and presence of 10^{-5} M of inhibitor (II-b)

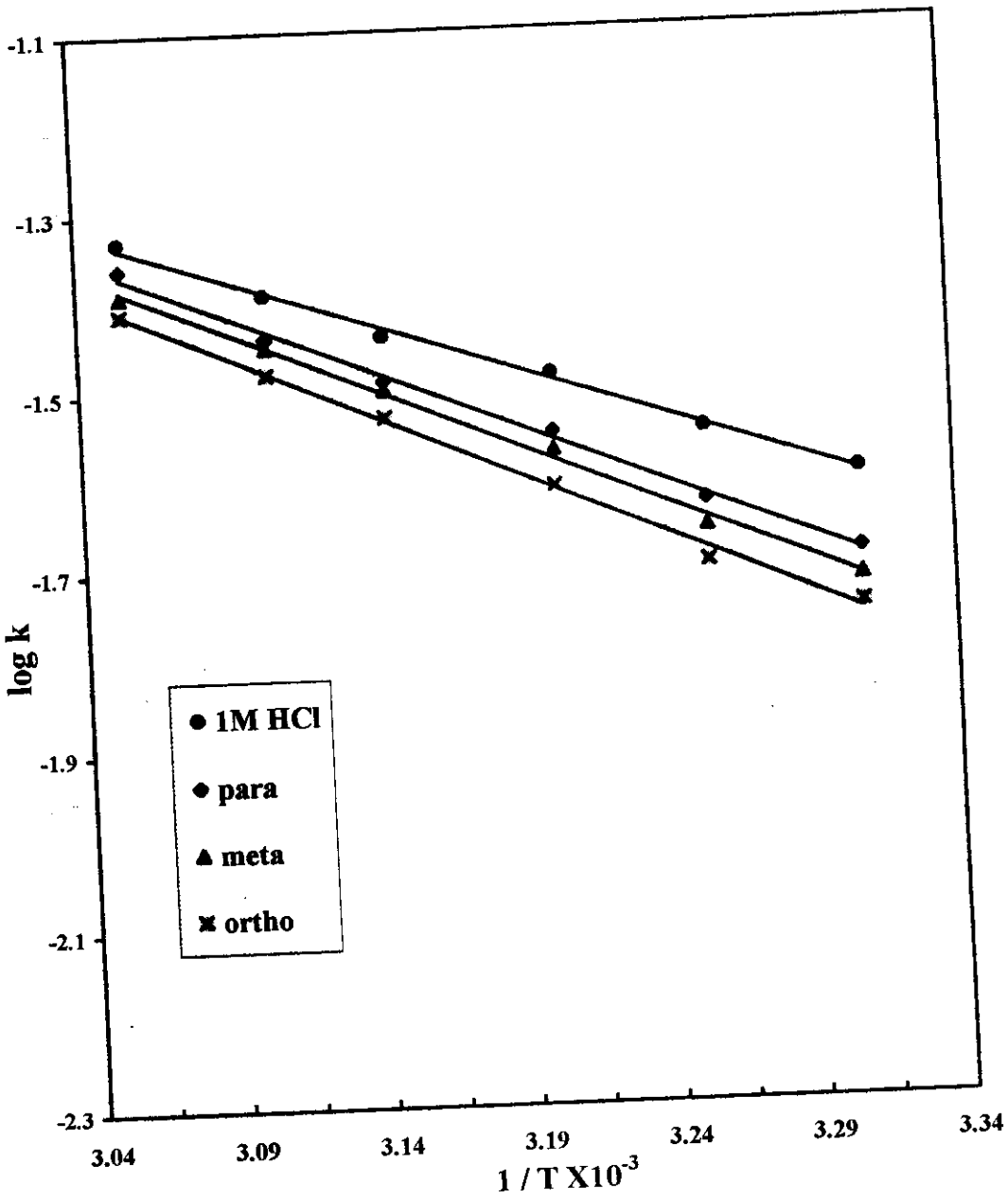

Fig (3.37): log K- 1/T curves for carbon steel dissolution in 1 M HCl in the absence and presence of 10^{-6} M of inhibitor (II-c)

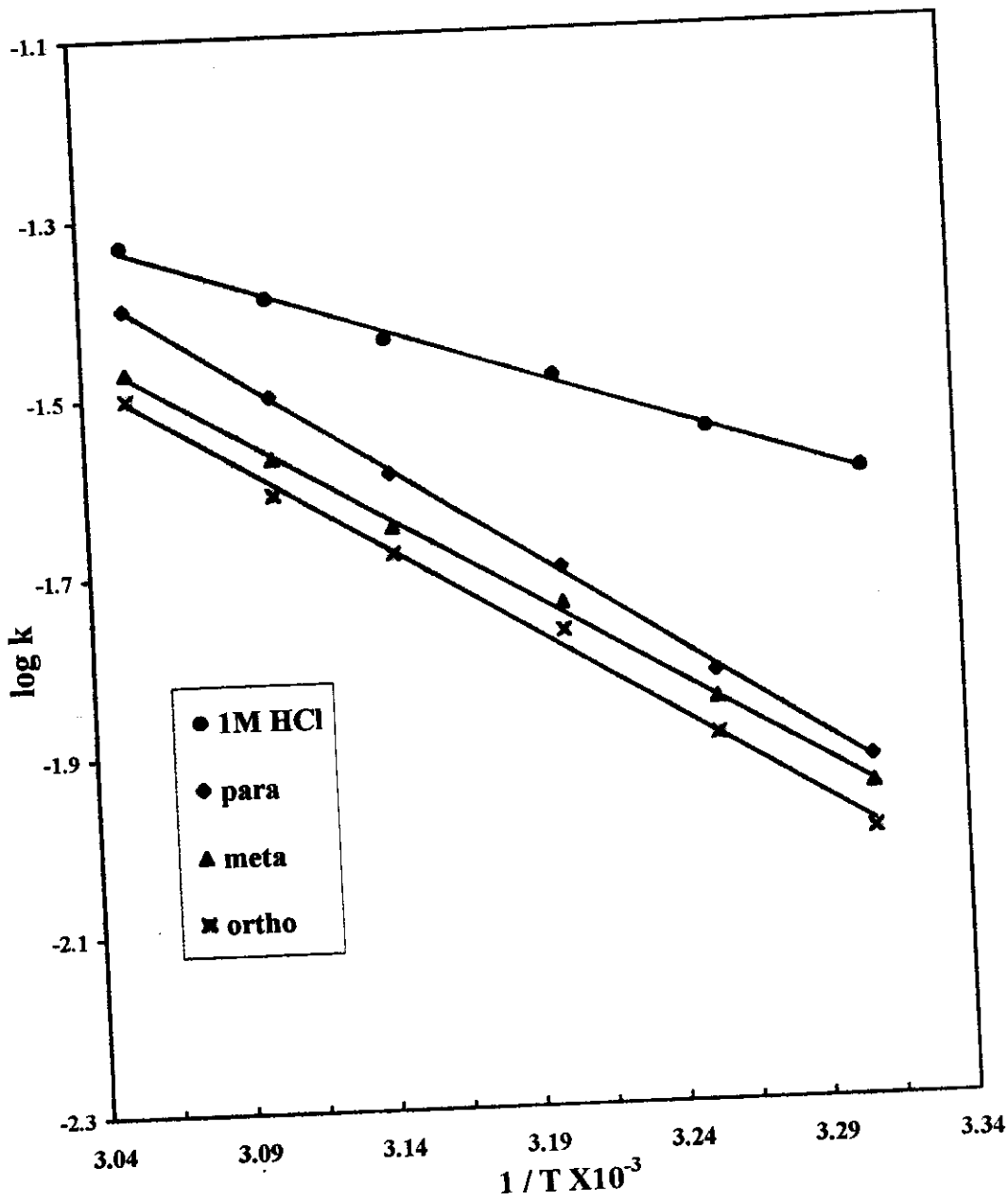

Fig (3.38): log K- 1/T curves for carbon steel dissolution in 1 M HCl in the absence and presence of 10^{-4} M of inhibitor (III-a)

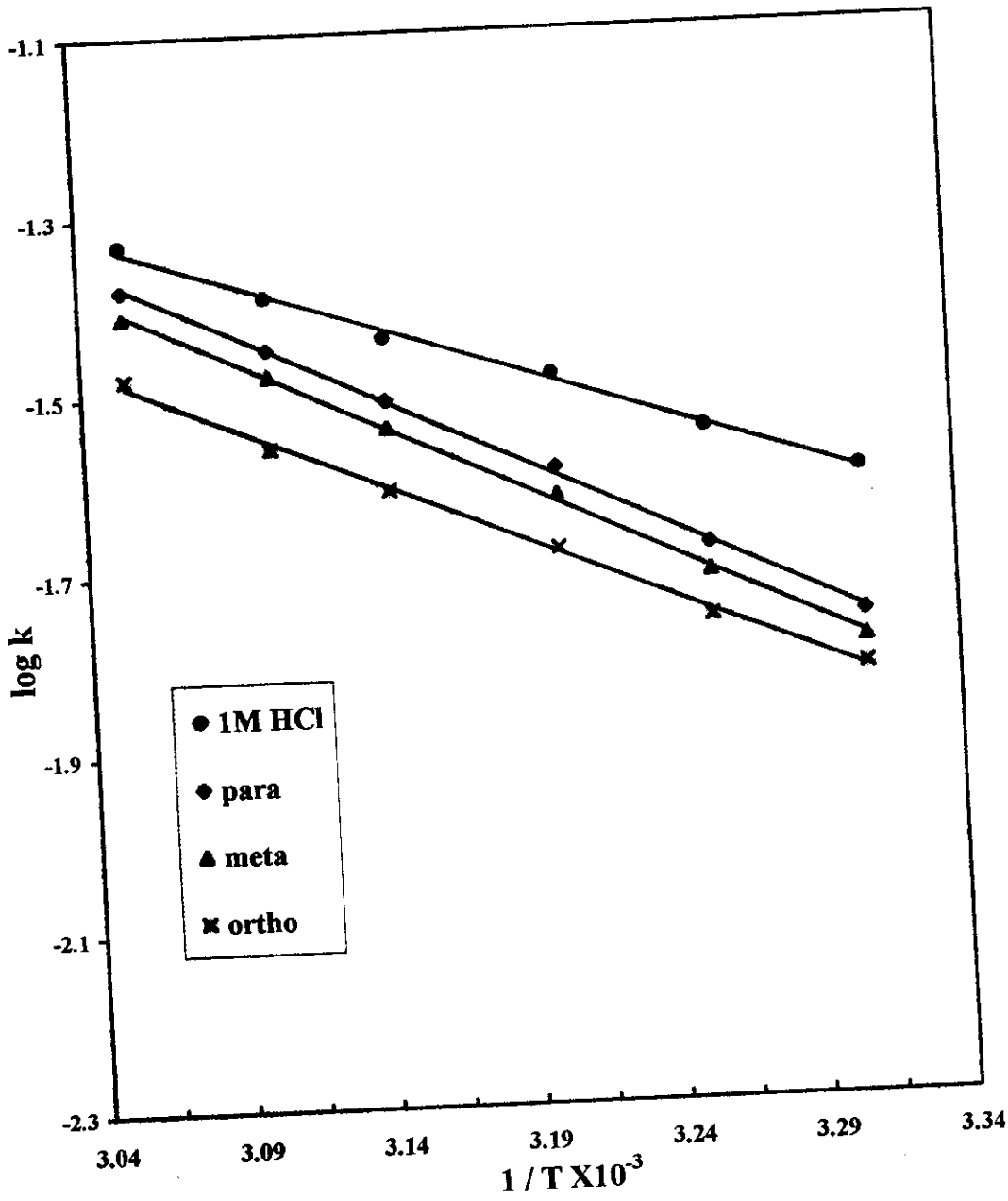

Fig (3.39): log K- 1/T curves for carbon steel dissolution in 1 M HCl in the absence and presence of 10^{-5} M of inhibitor (III-b)

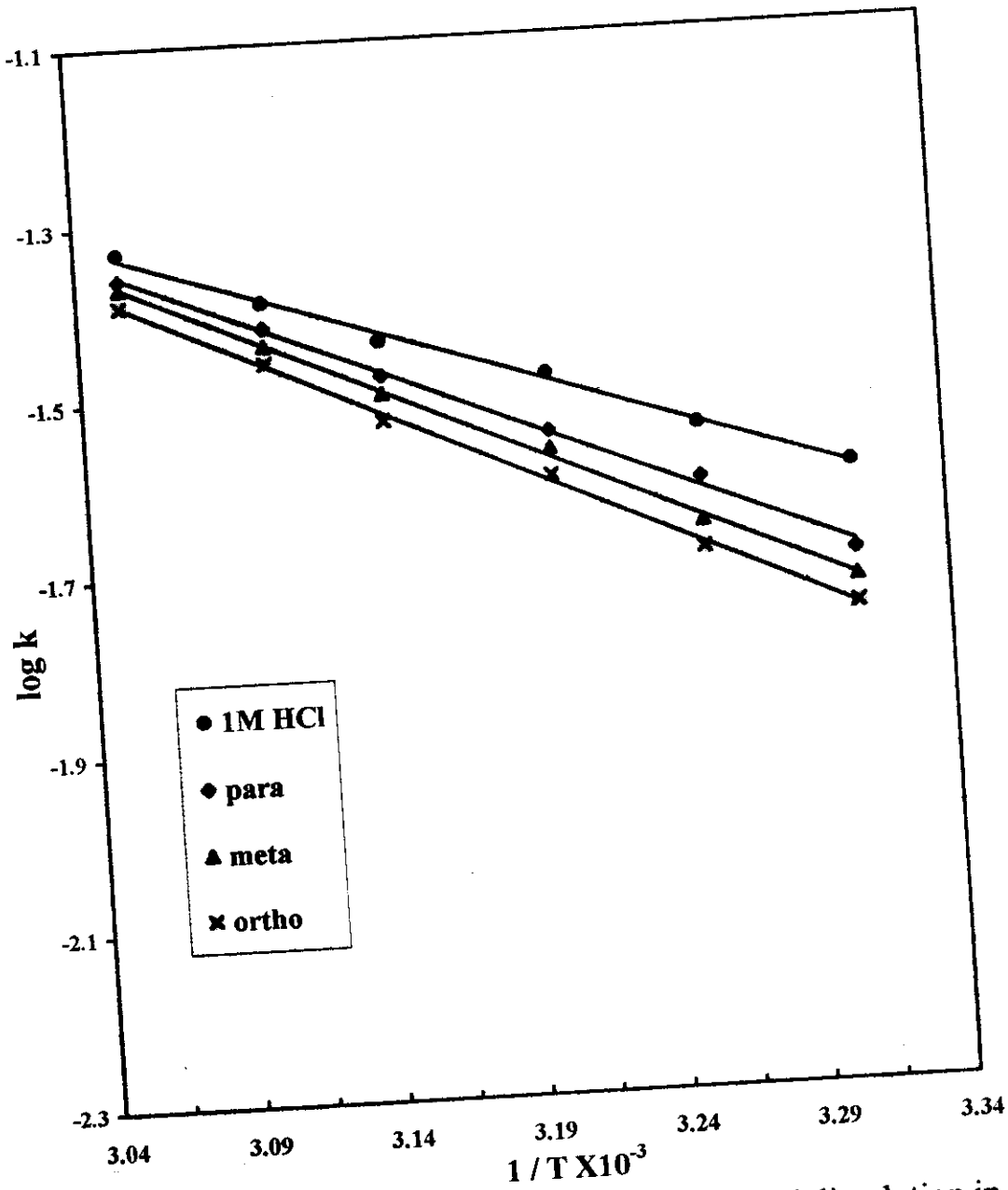

Fig (3.40): log K- 1/T curves for carbon steel dissolution in 1 M HCl in the absence and presence of 10^{-6} M of inhibitor (III-c)

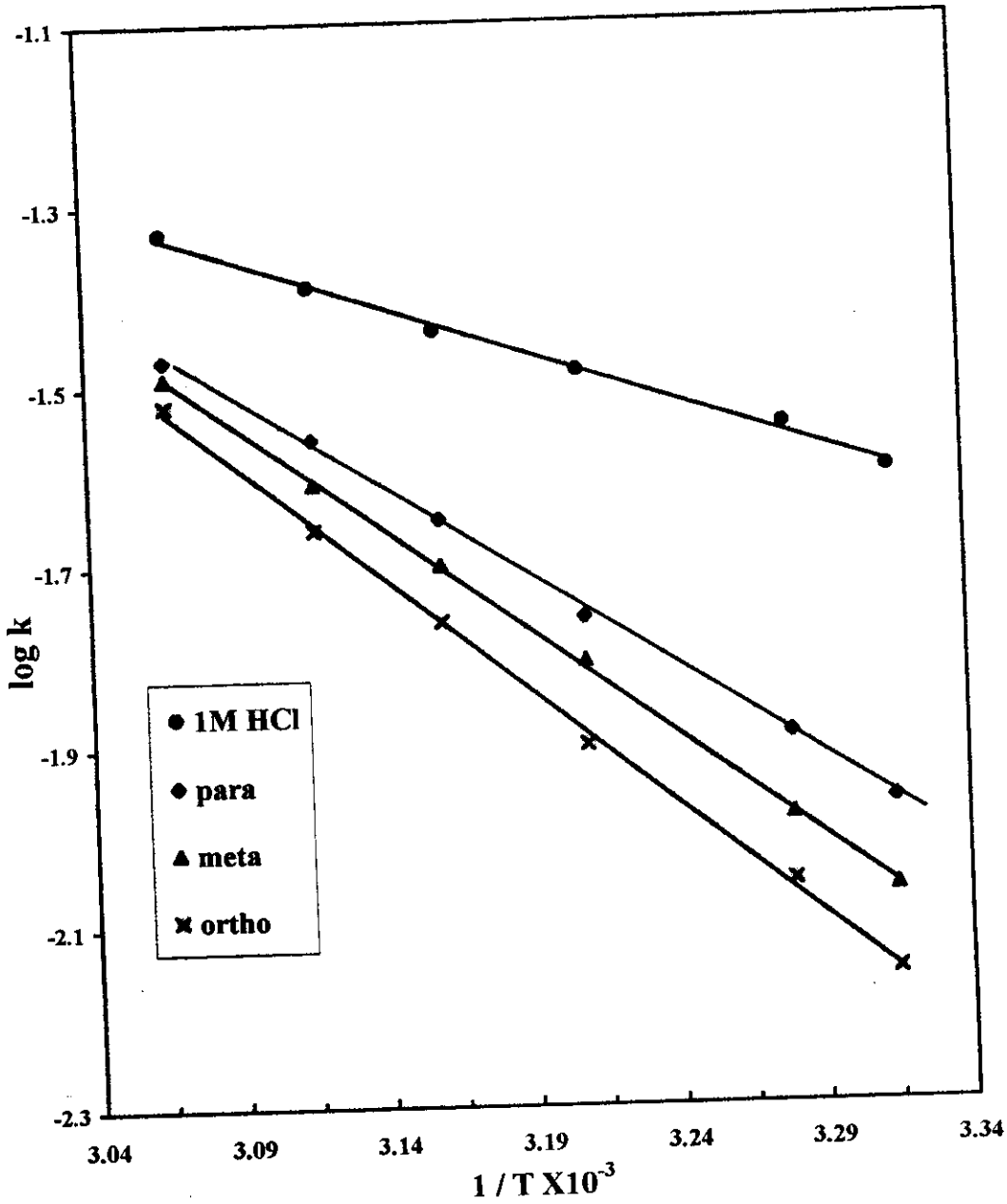

Fig (3.41): log K- 1/T curves for carbon steel dissolution in 1 M HCl in the absence and presence of 10^{-4} M of inhibitor (IV-a)

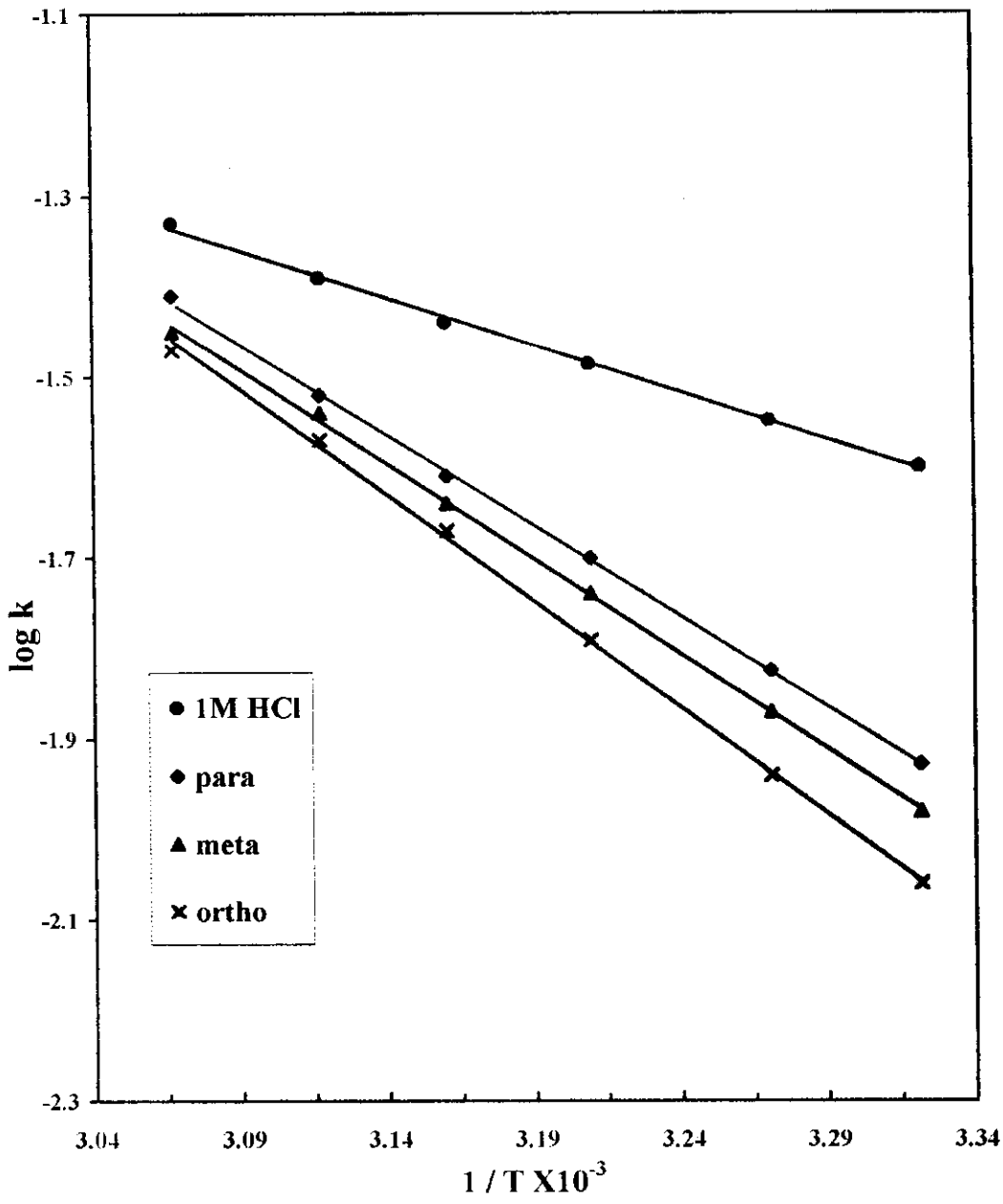

Fig (3.42): log K- 1/T curves for carbon steel dissolution in 1 M HCl in the absence and presence of 10^{-5} M of inhibitor (IV-b)

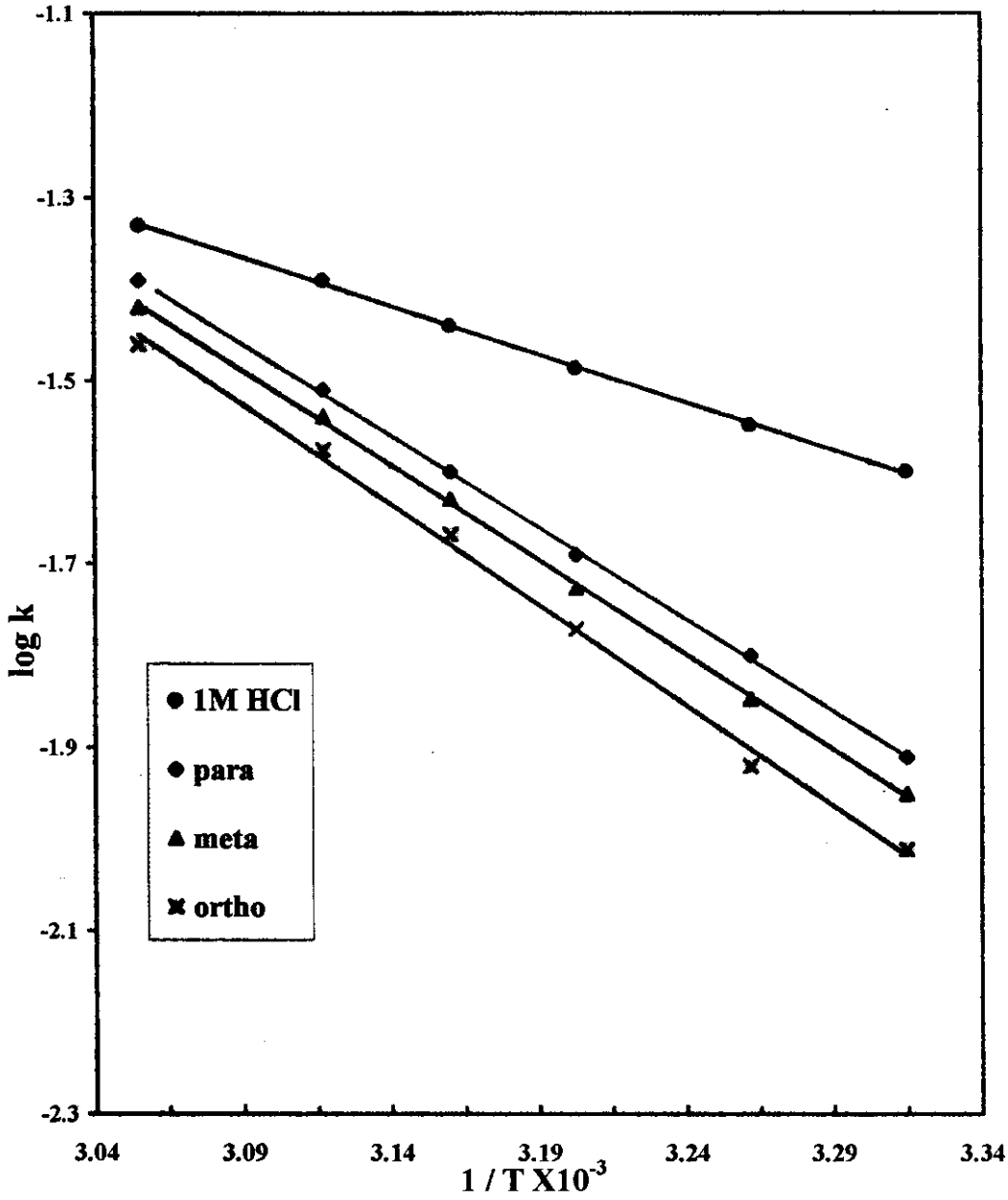

Fig (3.43): log K- 1/T curves for carbon steel dissolution in 1 M HCl in the absence and presence of 10^{-6} M of inhibitor (IV-c)

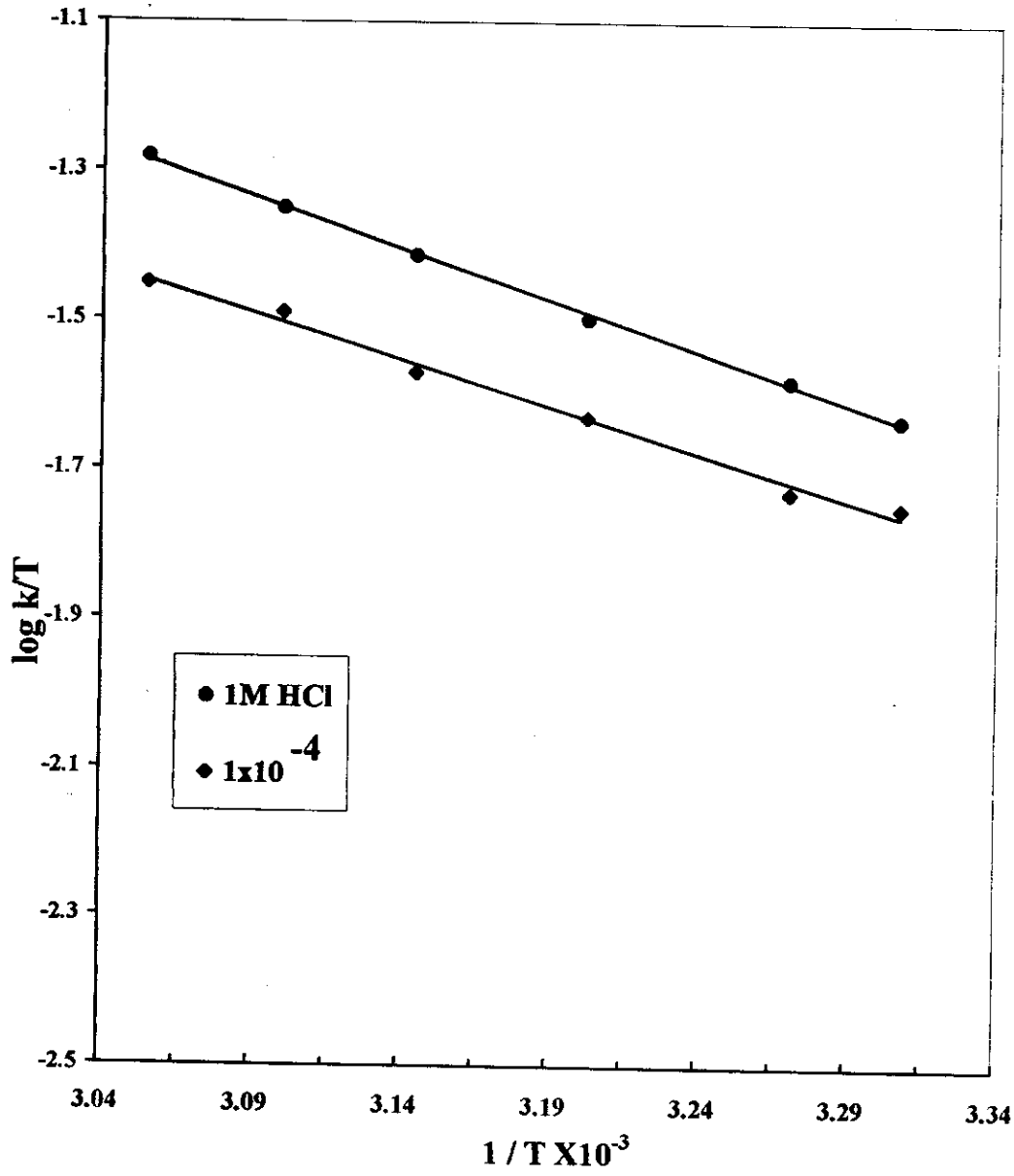

Fig (3.44): log K/T- 1/T curves for carbon steel dissolution in 1 M HCl in the absence and presence of $1x\ 10^{-4}$ M of inhibitor (I)

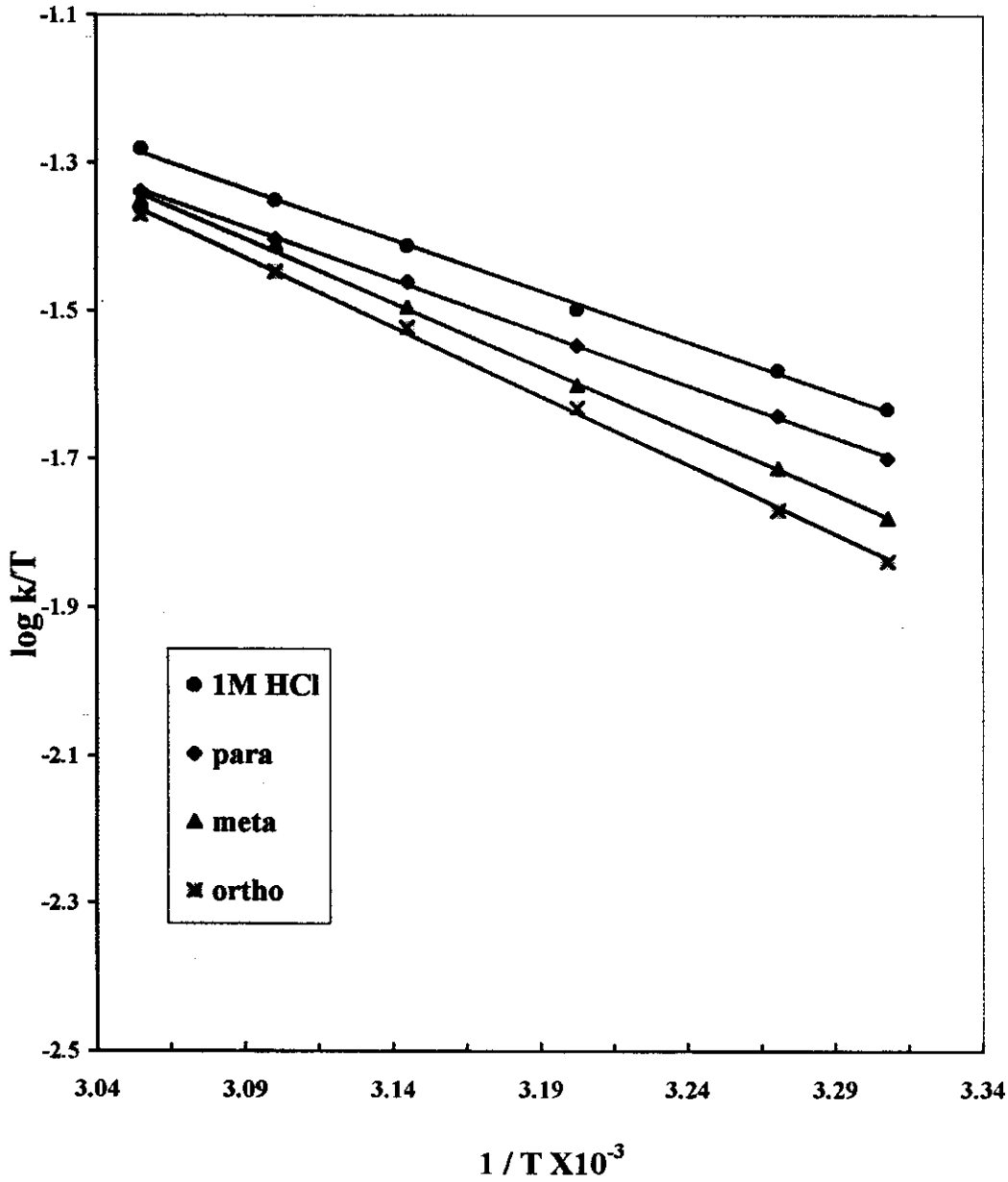

Fig (3.45): log K/T- 1/T curves for carbon steel dissolution in 1 M HCl in the absence and presence of 1x 10^{-4} M of inhibitor (II)

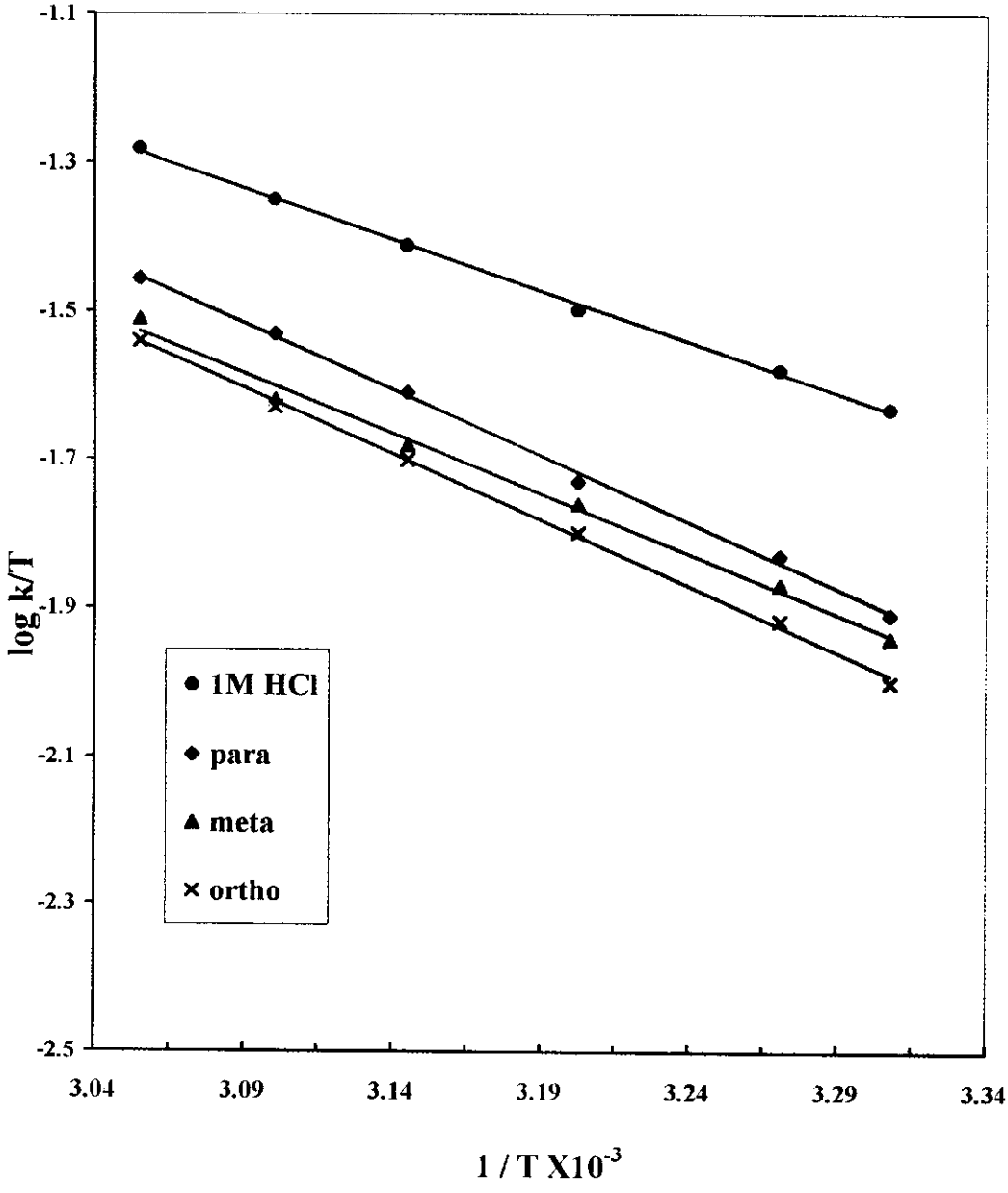

Fig (3.46): log K/T- 1/T curves for carbon steel dissolution in 1 M HCl in the absence and presence of 1x 10^{-4} M of inhibitor (III)

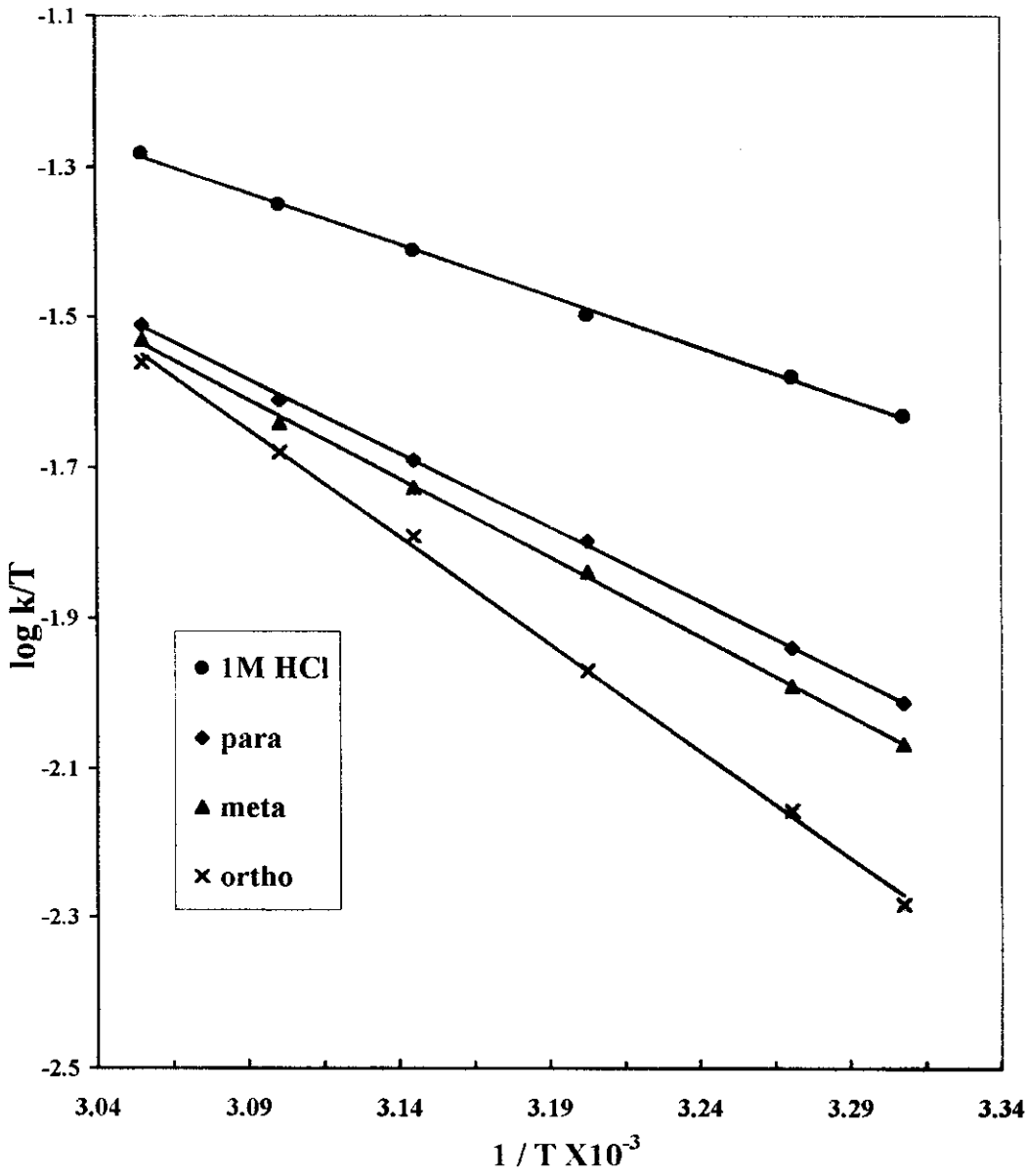

Fig (3.47): log K/T- 1/T curves for carbon steel dissolution in 1 M HCl in the absence and presence of 1x 10^{-4} M of inhibitor (IV)

Table (3.13): Effect of temperature on the inhibition efficiency of 10^{-4} M of inhibitors.

Temp. °C	% inhibition								
	II			III			IV		
	o-	m-	p-	o-	m-	P-	o-	m-	p-
30	73	69	68	74	70	61	83	80	77
35	62	55	50	63	62	51	72	66	66
40	58	50	46	52	50	42	64	45	54
45	48	40	36	43	40	34	53	40	48
50	39	30	27	33	30	27	45	32	35
55	26	20	16	23	20	18	35	30	28

Table (3.14): Effect of temperature on the inhibition efficiency of 10^{-5} M of inhibitors.

Temp. °C				% inhibition					
	II			III			IV		
	o-	m-	p-	o-	m-	p-	o-	m-	p-
30	59	54	48	60	57	54	77	72	66
35	48	37	55	51	49	46	57	53	56
40	37	34	33	42	35	34	42	44	46
45	28	25	22	30	28	26	31	40	38
50	20	19	17	22	20	19	26	30	28
55	11	10	99	12	10	8	17	26	12

Table (3.15): Effect of temperature on the inhibition efficiency of 10^{-6} M of inhibitors.

				% inhibition					
Temp. °C	II			III			IV		
	o-	m-	p-	o-	m-	p-	o-	m-	p-
30	52	48	40	55	49	44	69	58	55
35	41	36	32	38	35	30	49	46	39
40	31	27	20	32	31	27	36	34	32
45	21	18	15	26	23	19	30	28	26
50	12	16	12	17	15	10	25	20	18
55	7	8	5	10	8	7	12	10	8

Table (3.16): Activation parameter for the dissolution reaction of C-steel in presence of 10^{-4} M inhibitor in 1M HCl .

Inhibitor	Activation parameter			
	position	Ea° KJ mol^{-1}	ΔH° KJ mol^{-1}	$-\Delta S°$ J $mol^{-1}K^{-1}$
Free Acid		21.1	23.0	268
(I)		32.5	33.0	271
(II)	ortho	36.4	38.1	266
	meta	30.7	32.5	267
	para	28.7	29.3	267
(III)	ortho	38.3	38.4	264
	meta	36.4	35.7	264
	para	36.4	35.1	265
(IV)	ortho	46.0	44.8	263
	meta	44.0	43.7	263
	para	42.1	41.9	264